



Chapter 4

EXPERIMENTAL AND PRELIMINARY INVESTIGATION

Preparation of Tungsten Vanadium Oxide

Tungsten vanadium oxide was prepared by three methods

1. An equimolar mixture of V_2O_5 and WO_3 was heated in an evacuated quartz tube at $700^\circ C$ for one day and then annealed at $650^\circ C$ for one month. (25)

2. Sixty mole percent of an equimolar mixture of Na_2WO_4 and WO_3 and 40 mole percent of V_2O_5 were melted together in a platinum crucible at $1050^\circ C$ for 2 hours. The melt was cooled at the rate of $10^\circ C$ per hour to $700^\circ C$ after which it was left in the furnace to cool slowly to room temperature. The $Na_2W_2O_7$ was removed from the solidified melt by washing with concentrated sodium hydroxide solution to convert water insoluble $Na_2W_2O_7$ to soluble Na_2WO_4 . The mixture was then filtered and washed with distilled water until free alkali. (26)

3. The ground mixture consisting of equimolar ratio of V_2O_5 and WO_3 was contained in an opening quartz tube and heated with C_2H_2/O_2 flame. The product was heterogeneous. By iterative operation, grinding the product and reheating, a homogeneous product can eventually be obtained. The product was then sealed in a quartz ampoule. The ampoule was introduced in the step-freeze furnace (Fig. 4.1) at a temperature about $1075^\circ C$. (27)

The voltages of the furnace were controlled by a variac of range 0-250 volts. The voltages at distance 0,1,2,3,4 cm. from point A

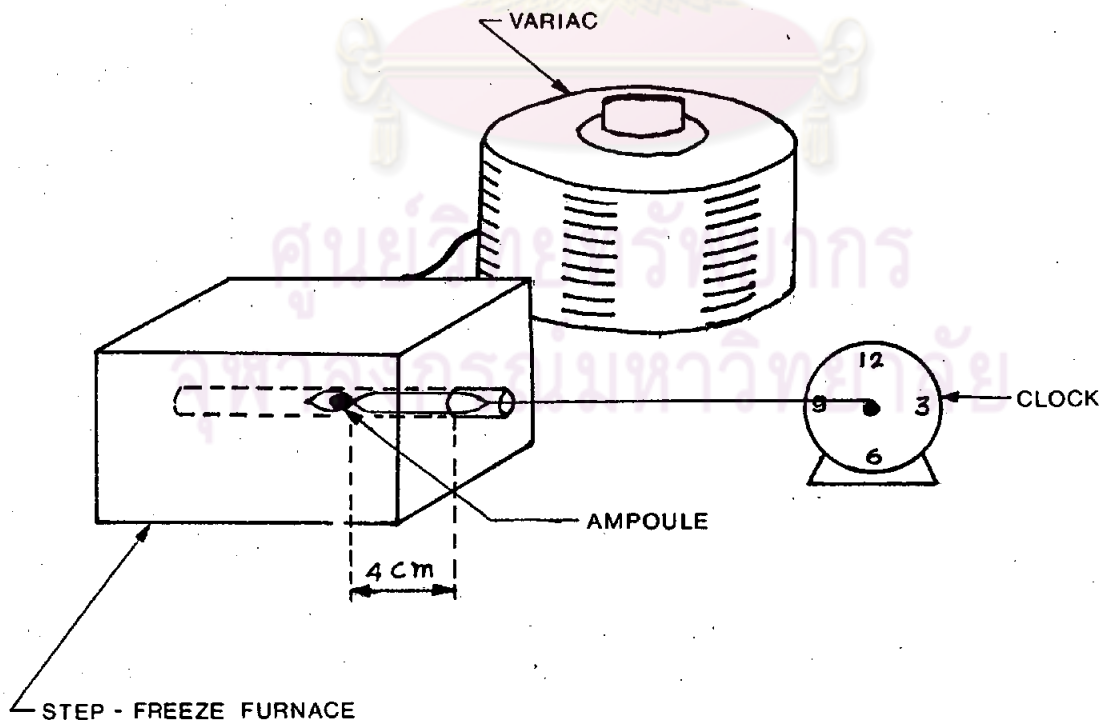
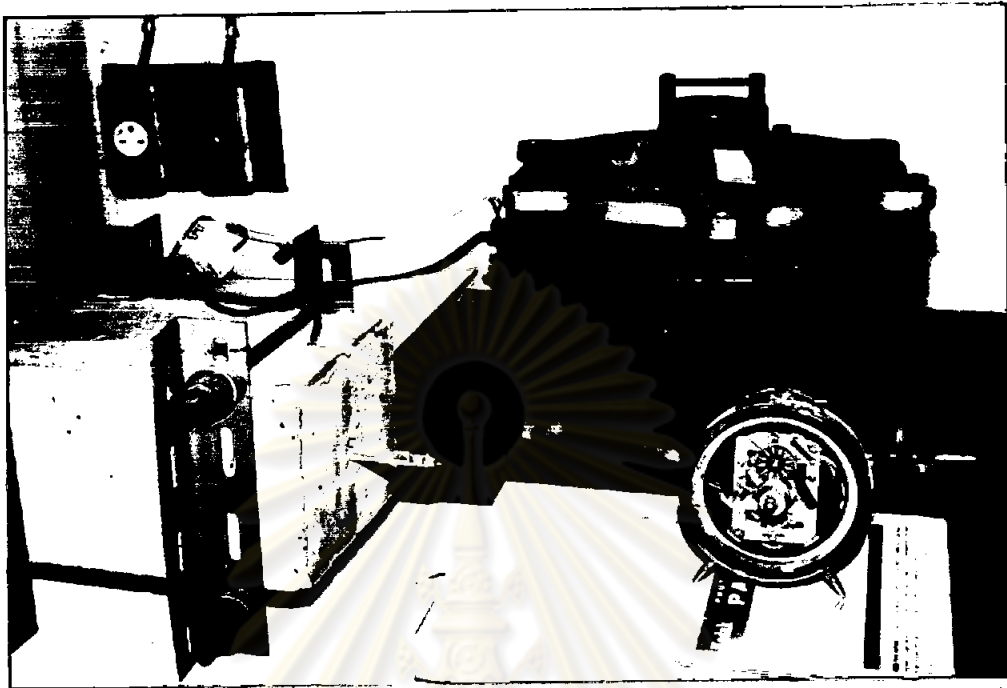


Fig. 4.1 The apparatus for the growth of single crystals of $W_3V_5O_{20}$

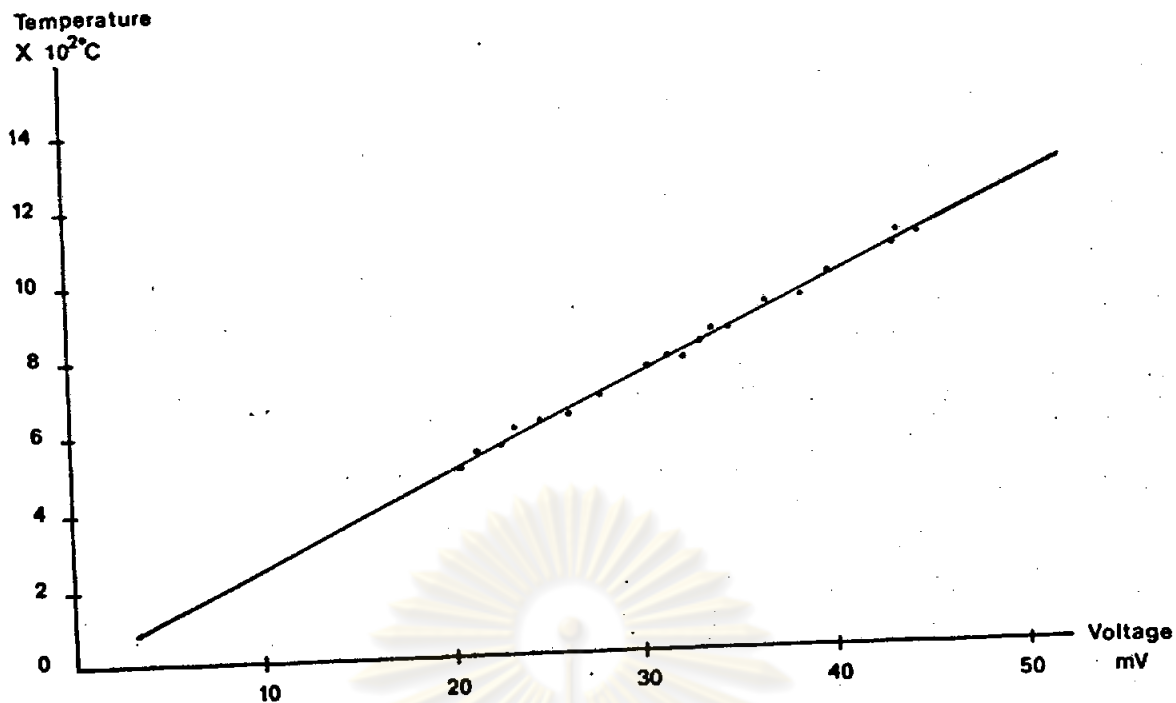


Fig. 4.2 Calibration curve plotted between voltages and temperatures of chromel-alumel thermocouple.

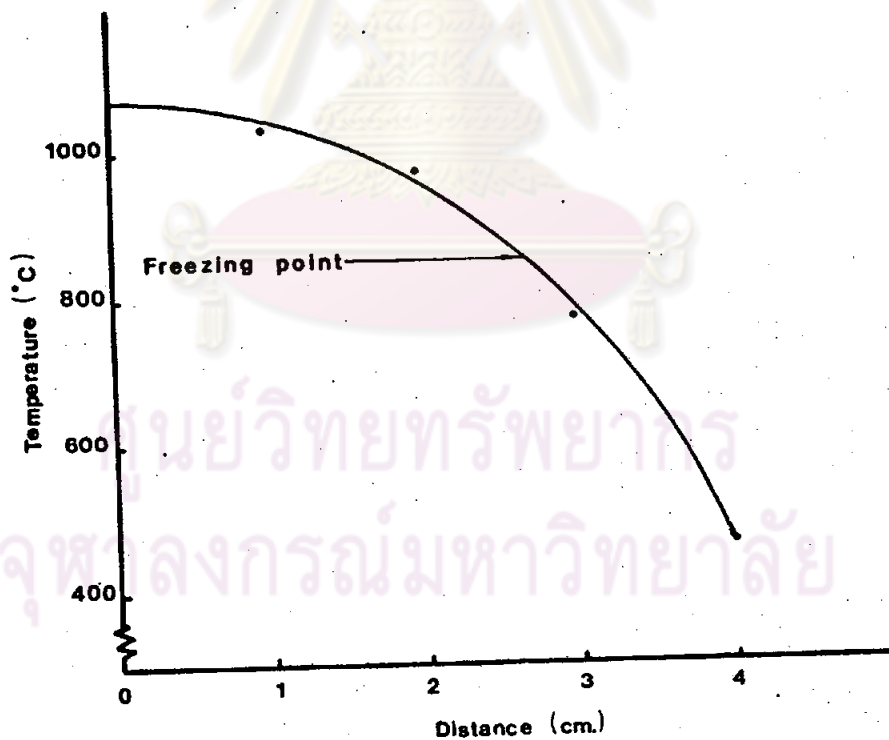


Fig. 4.3 The temperature profile of a step-freeze furnace used to prepare $W_3V_5O_{20}$ compound.

to the furnace opening point B were measured with alumel-chromel thermocouple and then converted to temperatures by using calibration curve of voltage temperature of the thermocouple. the calibration curve was shown in Fig. 4.2. The temperature gradient at the freezing temperature was $188^{\circ}\text{C}/\text{cm}$.

In Fig. 4.1 the ampoule was pulled slowly from point A, to point B which is in the direction of lower temperature by using driving mechanism from a clock. Fig. 4.3 shows the variation of temperature with pulling distance. The driving mechanism was built to provide 0.99 cm/hr . The method described above was modified from the Bridgeman technique⁽²⁷⁾.

The single crystals of tungsten vanadium oxide obtained by the first and the second methods were too small to study with X-ray diffraction but by the third method the crystals were big enough and have been used to study through out this work.

In addition to tungsten vanadium oxides which were black crystals, the yellow and brown samples were also obtained by the third method. The yellow, brown and black samples which were expected to be V_2O_5 , WO_3 and $\text{W}_3\text{V}_5\text{O}_{20}$ were identified by chemical analysis, measuring densities and powder method.

Chemical Analysis

The samples were separated into the three colour groups by using a microscope with 20 times magnifying power. Each group was mixed with a mixture of equal parts of Na_2CO_3 and K_2CO_3 the mixture was heated in a porcelain crucible for 10-15 minutes. After the melt cooled, distilled water was added. The solution was boiled and brought

to test for the vanadate and tungstate ion.

For testing tungstate ion, the solution was acidified with dilute acetic acid, and evaporated to expel CO_2 . The solution was divided into three parts. Dilute HCl was added to the first portion. The white precipitate of hydrated tungstic acid $\text{H}_2\text{WO}_4 \cdot \text{H}_2\text{O}$ was produced at room temperature. Upon boiling it was converted to yellow tungstic acid H_2WO_4 which was insoluble in dilute acids. The second portion was treated with dilute hydrochloric acid, a blue precipitate was produced after the addition of a little zinc. This was probably due to W_2O_5 or to WCl_3 . The last portion was treated with AgNO_3 solution. The pale yellow precipitate of the ammonia soluble silver tungstate was obtained. It was decomposed by nitric acid with the formation of white hydrated tungstic acid. Hence it was confirmed that the filtrate was containing tungstate ion.

For testing the presence of vanadate ion, the solution was divided into three parts. Zinc powder was added to the first portion. The solution turned at first blue (vanadyl salt-quadrivalent vanadium), then green (tervalent vanadium) and finally violet (bivalent vanadium). The second portion was treated with ammonium sulphide solution. There was vanadium sulphide V_2S_5 which was incompletely precipitated, and the filtrate had blue colour. The precipitate was soluble in solutions of alkalis, alkali carbonates and sulphides. Lead acetate solution was added to the third portion. The yellow precipitate of lead vanadate, turning white or pale yellow on standing, was obtained. The precipitate was soluble in dilute nitric acid. All of the tests mentioned above confirmed the presence of the vanadate ion or the vanadium ion.

The black crystals gave positive test for tungstate ion and vanadate ion, the brown crystals gave positive test only for tungstate ion and the yellow crystals gave positive test only for vanadate ion. Therefore, the black precipitate was composed of VO_3^- or V^{5+} and $\text{WO}_4^{=}$. The brown was composed of $\text{WO}_4^{=}$ whereas V^{5+} formed the yellow one.

These indicated that the black was tungsten vanadium oxide, the brown was WO_3 and the yellow was V_2O_5 . Such indications were confirmed by the X-ray powder diffraction patterns described later.

Density Measurement

The density of tungsten vanadium oxide was measured by using the method of Archimedes.

Tungsten vanadium oxide is insoluble in water. The density (ρ) was calculated from the formula

$$\rho = \frac{W \text{ in air}}{W \text{ in air} - W \text{ in water}}$$

The average density of tungsten vanadium oxide at 25°C was found to be $5.10 \pm .03 \text{ g/cm}^3$. The list of density measurements was shown in Table 4.1

The density of brown samples at 25°C was found to be $7.06 \pm .02 \text{ g/cm}^3$ with the method of Archimedes. For the yellow ones, the density at 25°C was measured by Floatation method. The three specimens of the yellow were immersed in the mixed solution of water, thallos malonate, thallos formate. It was found that the specimens neither rose nor sank in the mixed solution of density 3.28 g/cm^3 . This showed that the density of the yellow samples was 3.28 g/cm^3 .

Table 4.1 Densities of $W_3V_5O_{20}$ and necessary parameters for determining densities

No. of measuring	W in air (g)	W in air - W in water (g)	density (g/cm ³)
1	0.1932	0.0377	5.12
2	0.1930	0.0379	5.09
3	0.1927	0.0381	5.06
4	0.1920	0.0378	5.08
5	0.1925	0.0375	5.13
			ρ ave = 5.10±.03

The densities of WO_3 and V_2O_5 from CRC Handbook of chemistry and physics (1985-1986) are 7.10 and 3.34 g/cm³ respectively. Therefore the brown, yellow samples should be WO_3 and V_2O_5 respectively.

X-Ray Diffraction Photographs

The X-ray diffraction photographs in common use can be divided into two classes, i.e, power photographs and single-crystal photographs.

A powder photograph of $W_3V_5O_{20}$ was taken by using Guinier-Hägg focusing camera and mainly used for refinement of the unit cell dimension. The WO_3 and V_2O_5 compounds were used to take powder photographs for identification purpose only.

The single crystal structure of $W_3V_5O_{20}$ was studied by using oscillation, rotation, Laue, Weissenberg and precession photographs.

1. Powder photographs

The X-ray powder pattern for tungsten vanadium oxide was recorded in a Guinier-Hägg-type focussing powder camera (Philip XDC-700) with $\text{CuK}\alpha_1$ radiation ($\lambda = 1.540598 \text{ \AA}$) using silicon 99.9% ($a = 5.431065 \text{ \AA}$) as internal calibration standard. The powder photograph was taken at 28°C for approximately one hour. The positions of diffraction lines on the photographs were measured with NORELCO film-measuring device.

The above procedure was also used to obtain the X-ray powder pattern for the brown samples. Then the obtained powder photographs of the brown samples were compared with that of known WO_3 which was recrystallized by melting at 800°C in an evacuated quartz tube.

In addition, the above procedure but without silicon was also repeated to get the X-ray powder patterns for the brown samples and for known V_2O_5 which was recrystallized by melting at 800°C in an evacuated quartz tube.

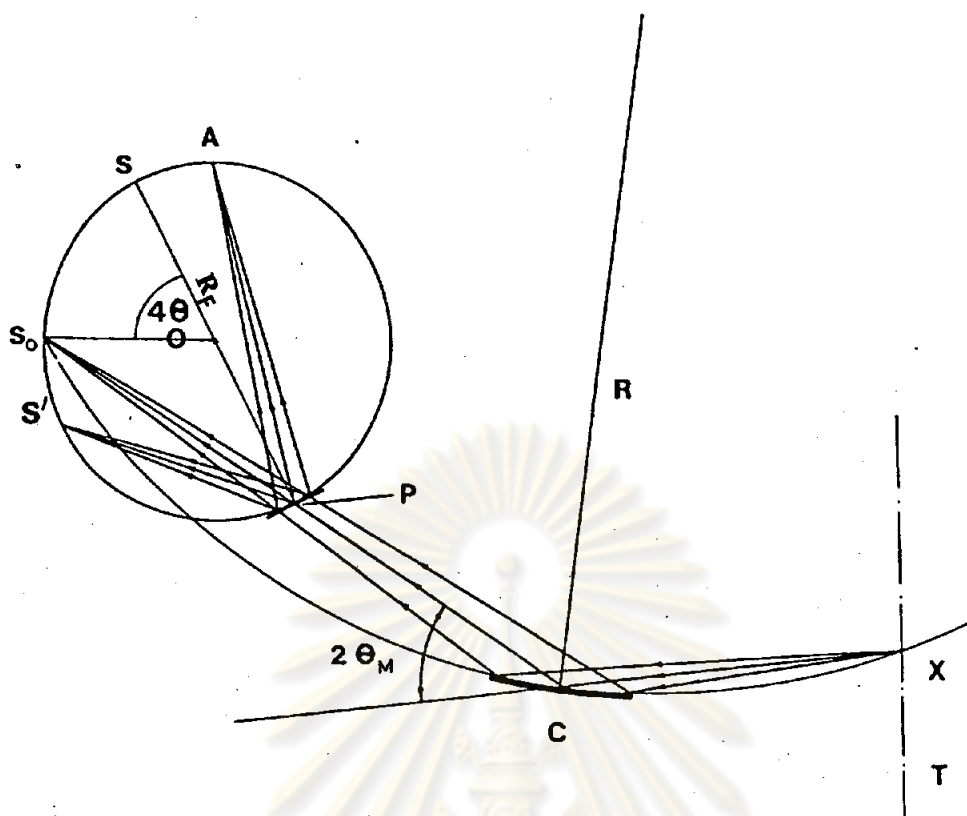
The principle of Guinier-Hägg camera and X-ray powder photographs of all compounds were shown in Fig. 4.4 and Fig. 4.5 respectively.

From Fig. 4.4, The Bragg angle can be obtained obviously as

$$\theta = \frac{180}{\pi R_F} (S - S_0) \text{ in degree} \dots\dots\dots 4.1$$

$$\text{or } \theta = K (S - S_0) \dots\dots\dots 4.2$$

$$\text{where } K = \frac{180}{\pi R_F}$$



- X Line focus of X-ray tube
- T Axes of X-ray tube
- C Centre (axis of rotation) of monochromator crystal
- R Radius of monochromator focussing circle
- O Centre of film cylinder in holder
- P Centre of powder sample
- S₀ Focal line (Primary beam)
- A&S' Examples of diffraction lines in the case of "addition" and "subtraction" respectively
- $2\theta_M$ Angle of deviation at the monochromator = angle between reflected beam CS_0 and primary beam XC
- S Diffraction line
- R_F Radius of film cylinder

Fig. 4.4 Diagram showing the principle of the Guinier method.

Qualitative analysis by JCPDS* powder Diffraction File

The principle of the identification of substance by X-ray powder diffraction is based on the fact that each crystalline substance produces its own characteristic pattern which is different from the pattern given by other substances.

The procedure for identifying a powder diffraction pattern consists of measuring the diffraction angles and the intensities, calculating the spacing, d of the reflecting planes, choosing the 3-8 strongest lines arranged in decreasing order of their relative intensities, and then using the JCPDS powder Diffraction File to identify that compound.

The sequence for using the Powder Diffraction File of unknowns containing only one component is as follows. First, the correct Hanawalt group are searched for the strongest line, it may be necessary to consult two or three Hanawalt groups if the value of the strongest line close to the limit between them. Second, the second column in the appropriate Hanawalt group is taken into consideration to search for a match with the second strongest line. Third, the entry which also show a match for the third strongest line is selected and then the compound might be known. If there are two sets of entries which have d values that are reasonably close to the observed values, they may be distinguished via other data such as the relative intensities of the reflections.

For unknowns containing a mixture, the procedure described in the preceding section is used in principle whether the powder contains

* JCPDS = Joint Committee on Powder Diffraction Standards

one or several components. If the three strongest lines of a diffraction pattern do not lead to an identification, the sample may be a mixture of compound. It is necessary to select properly the three most intense reflections for each component

The tungsten vanadium oxide was identified by comparing with the powder data of Kihlberg.⁽⁵⁾ The intensity of each diffraction line was estimated visually. The values of S_0 , S and $(S-S_0)$ were obtained from the Guinier film where S_0 is the reading in mm. of the reference primary line and S is the reading in mm. of each diffraction line including silicon lines. The correction of observed data was calculated by calibration with the standard diffraction lines of silicon. The calculation was performed by using program GUINE⁽³²⁾ to obtain the corrected powder diffraction data as shown in Table 4.2

Table 4.2 The values of d_o and d_{ref} of the powder diffraction lines.

I	$S - S_0$ (mm)	θ (degree)	d_o	d_{ref}	I_{ref}
M	25.35	7.2479	6.102	6.120	M
VS	39.30	11.2367	3.950	3.949	VS
VS	43.65	12.4806	3.562	3.572	VS
M	51.15	14.6252	3.051	3.059	M
S	56.95	16.2838	2.747	2.754	S
S	59.05	16.8843	2.652	2.653	S
W	85.30	24.3923	1.866	1.868	S
W	95.00	27.1075	1.687	1.687	W
VW	96.10	27.4822	1.669	1.668	VW
S	102.10	29.1990	1.579	1.580	S

The X-ray powder data of brown samples were identified by using the JCPDS powder Diffraction File. The results indicated that this compound is WO_3 . The values for this calculations are listed in

Table 4.3

Table 4.3 The powder diffraction data of brown crystal (WO_3) comparing with WO_3 from Powder Diffraction File card No.20-1324.

I	$S - S_0$ (mm.)	θ (degree)	d_o	d_{ref}	I_{ref}
VS	40.42	11.5478	3.85	3.85	100
M	41.32	11.8052	3.76	3.75	65
VS	42.17	12.0483	3.69	3.69	95
VW	45.47	12.9923	3.43	3.43	2
W	58.27	16.6547	2.687	2.686	35
W	58.77	16.7980	2.665	2.662	35
M	59.52	17.0126	2.633	2.633	50
VW	73.22	20.7626	2.173	2.173	16
VW	79.27	22.6665	1.998	1.998	6
VW	84.63	24.1983	1.879	1.878	10
VW	87.27	24.9670	1.825	1.820	10
VW	88.33	25.2577	1.805	1.806	16
VW	93.58	26.7608	1.711	1.712	10
VW	94.97	27.1617	1.687	1.688	16
VW	95.77	27.3907	1.674	1.674	10
VW	96.58	27.6198	1.662	1.665	16
VW	97.63	27.9204	1.645	1.645	6
VW	106.42	30.4396	1.520	1.522	10
VW	108.86	31.1353	1.489	1.486	6

d_{ref}, I_{ref} obtained from the JCPDS card No. 20-1324

From Fig. 4.5 the powder photographs of yellow and brown samples were compared with known V_2O_5 and known WO_3 which were recrystallized by heating at 800°C in evacuated quartz tubes. It was found that the diffraction lines of powder photographs of yellow and brown samples were matched with the lines of powder patterns of V_2O_5 and WO_3 respectively. These indicate that yellow and brown samples were V_2O_5 and WO_3 respectively.

Determination of accurate unit cell dimension

The unit cell dimensions of tungsten vanadium oxide were refined by least square method using program CELNE⁽³²⁾

The data used for the refinement were 26 observed $\sin^2\theta_{hkl}$ and the Miller indices hkl . The Miller indices were obtained by calculation of $\sin^2\theta$ by using the preliminary cell dimension from Kihlberg's. The formula for indexing monoclinic crystal with b unique axis is

$$\sin^2\theta_{hkl} = Ah^2 + Bk^2 + Cl^2 - D_{hl}$$

where

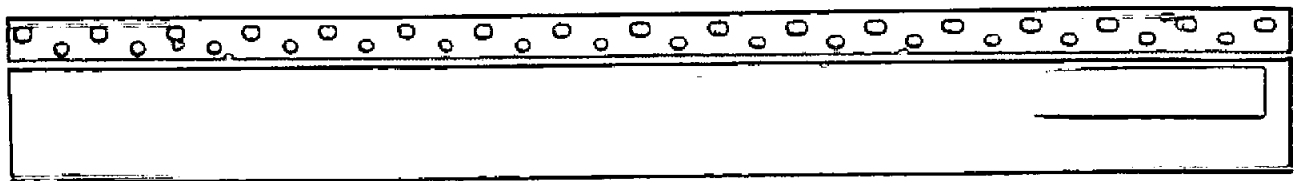
$$A = \frac{\lambda^2}{4a^2 \sin^2\beta}$$

$$B = \frac{\lambda^2}{4b^2}$$

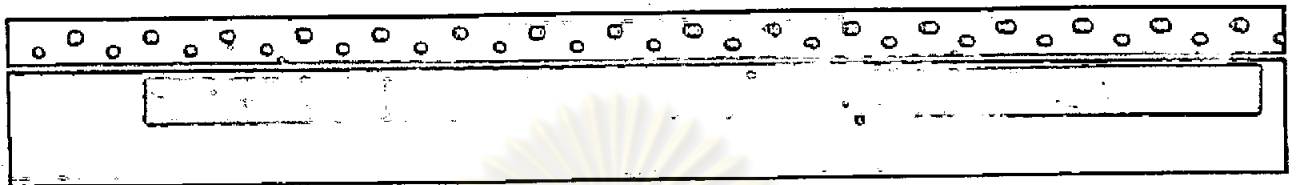
$$C = \frac{\lambda^2}{4c^2 \sin^2\beta}$$

$$D = \frac{\lambda^2}{2ac \sin^2\beta}$$

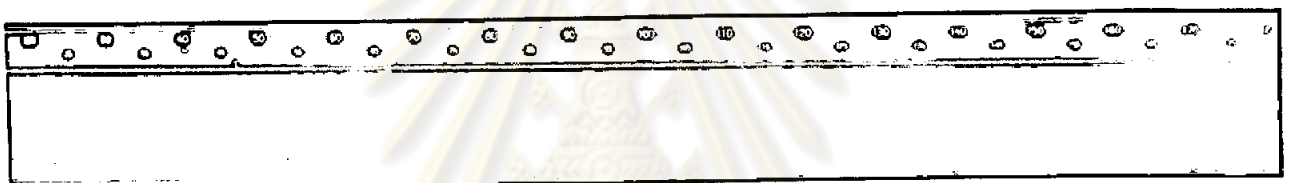
The results of refinement are shown in Table 4.4



(a)



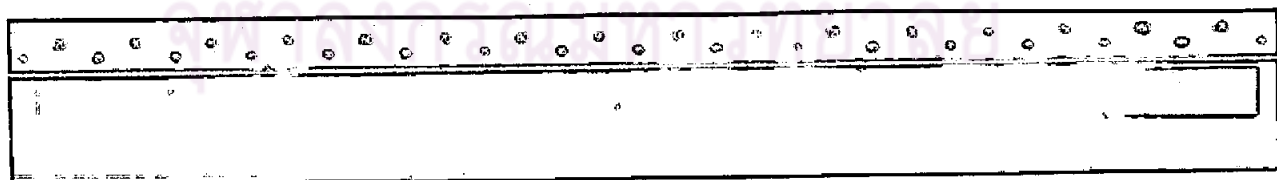
(b)



(c)



(d)



(e)

Fig. 4.5 Powder photographs of three compounds obtained from the third method of those preparations, comparing to known V_2O_5 and WO_3 :
 (a) yellow samples (b) V_2O_5 (laboratory reagents, EDE chemical Ltd.) (c) brown samples (d) WO_3 (Laboratory reagents, EDE chemical Ltd.) (e) black samples expected to be $V_2V_2O_{10}$

Table 4.4 Powder diffraction data for $W_3V_5O_{20}$. $\Delta = \sin^2 \theta_o - \sin^2 \theta_c$

I	d_o (Å)	hkl	$\sin^2 \theta_o \times 10^6$	$\sin^2 \theta_c \times 10^6$	$\Delta \times 10^6$
M	6.1056	400	15920	15935	-15
VS	3.9530	001	37970	38030	-60
VS	3.5644	220	46700	46770	-70
S	3.0508	800	63750	63741	9
S	2.7472	620	78620	78641	-21
S	2.6522	$\bar{2}21$	84360	84359	1
S	2.4331	230	100230	100253	-23
S	2.6284	611	85890	85906	-16
M	2.2551	$\bar{9}01$	116680	116715	-35
W	2.0383	$\bar{8}21$	142810	142792	18
W	1.9710	$\bar{1}02$	152730	152675	55
VW	1.8745	$\bar{6}31$	168870	168829	41
S	1.8652	$\bar{3}12$	170550	170456	94
S	1.7319	$\bar{7}02$	197830	197832	-2
W	1.6871	$\bar{7}12$	208480	208528	-48
VW	1.6692	$\bar{9}31$	212960	212985	-25
W	1.6448	802	219330	219394	-64
VW	1.6005	$\bar{1}0\ 3\ 1$	231640	231687	-47
V	1.5897	15 1 0	234810	234786	24
S	1.5790	14 2 0	237990	237993	-3
VW	1.4802	10 4 0	270830	270741	89
VW	1.4622	11 0 2	277510	277488	22
VW	1.4268	14 3 0	291480	291476	4
VW	1.4147	16 0 1	296490	296527	37
W	1.3223	16 2 1	339370	339313	57

The final cell parameters obtained were $a = 24.412 (2)$,
 $b = 7.4479 (8)$, $c = 3.9506 (3) \text{ \AA}$, $\beta = 91.028^\circ (7)$, $v = 718.194 \text{ \AA}^3$.

2. Single-crystal photographs by X-ray diffraction

A crystal which is satisfactory for collecting X-ray diffraction data must possess uniform internal structure called a single crystal. It should have proper size and shape and not be twinned or composed of microscopic subcrystals.

To obtain satisfactory single crystals, $W_3V_5O_{20}$ crystals were first examined from a microscope with magnifying power 20 times. The suitable crystals which were chosen, have particularly uniform or well-formed external faces. The diffraction pattern from those should give the reflections which are single spots and should be indexable in terms of a single three-dimensional lattice.

Two single crystals of $W_3V_5O_{20}$ were used for structure determination. A selected crystal mounted along the b-axis was a rectangular prism truncated at one corner as illustrated in Fig. 4.6. The other crystal mounted along c-axis was a rectangular prism as shown in Fig. 4.7

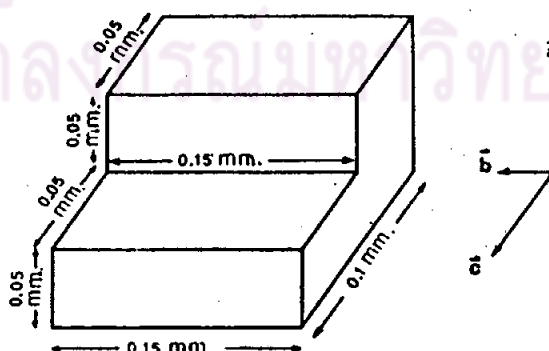


Fig. 4.6 A rectangular prism truncated at one corner

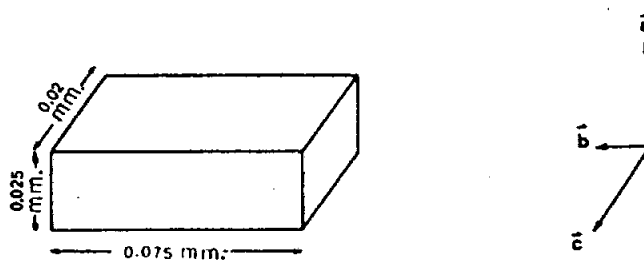


Fig. 4.7 A rectangular prism

Oscillation and rotation photographs

Oscillation and rotation photographs are generally used for three purposes : to align crystals, to measure the cell edge along the axis of rotation, and to obtain preliminary information about crystal symmetry.

A nonius Weissenberg camera of diameter 57.3 mm. was used in this experiment. The axes of the two crystals were first set normal to the beam by using 15° oscillation photographs. The crystal mounted along "b" as rotation axis, were used to take an oscillation photograph (Fig. 4.8) with CuK_α - radiation and a rotation photograph (Fig. 4.9) with Cu-radiation. For the crystal mounted along "c" as rotation axis, an oscillation photograph (Fig. 4.10) and a rotation photograph (Fig.4.11) were taken with Ni-filtered CuK_α - radiation ($\lambda_{\text{K}\alpha}=1.5418 \text{ \AA}$)

The X-ray tubes, Mo-target was run at 50 KV 14 MA and Cu target at 40 KV, 30 mA throughout the experiment.

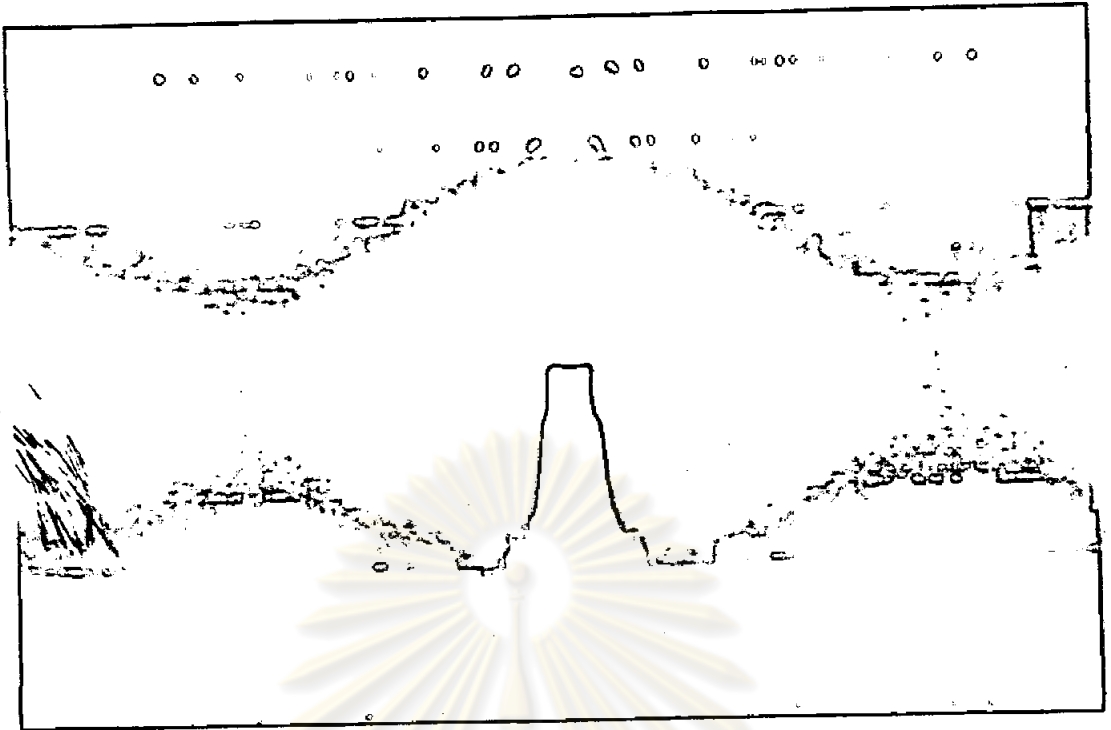


Fig. 4.9 Rotation photograph of [010] as rotation axis,
Cu. - radiation. Exposed 24 hr.

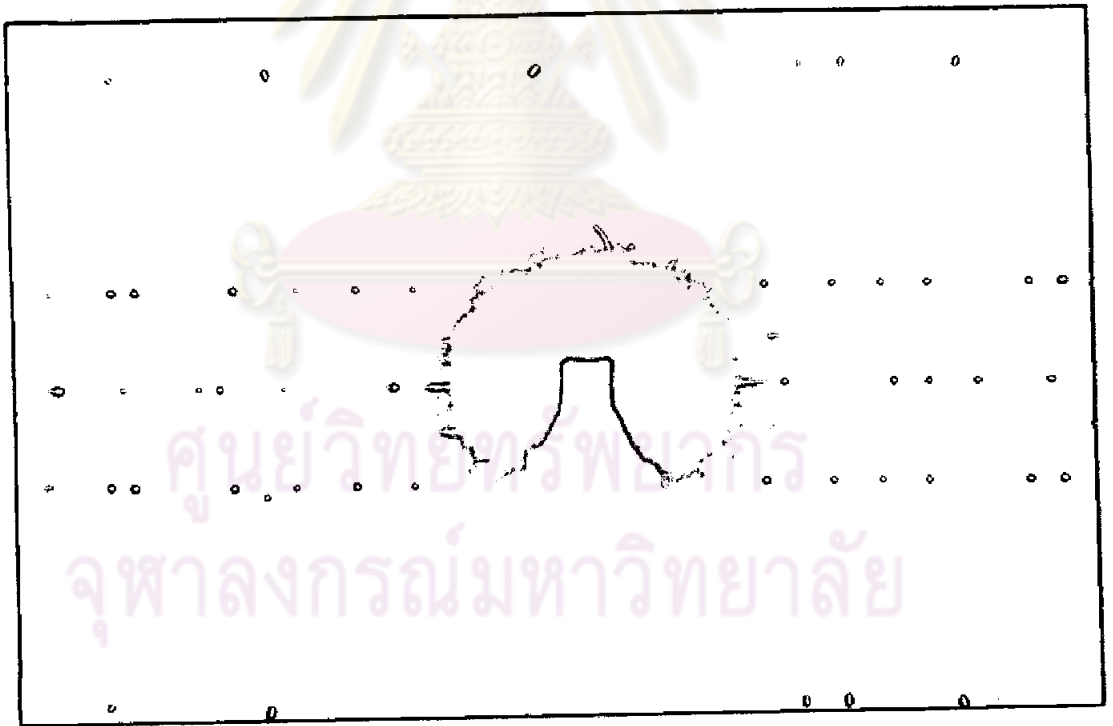


Fig. 4.8 Oscillation photograph of [010] as rotation axis,
CuK_α - radiation. Exposed 24 hr.

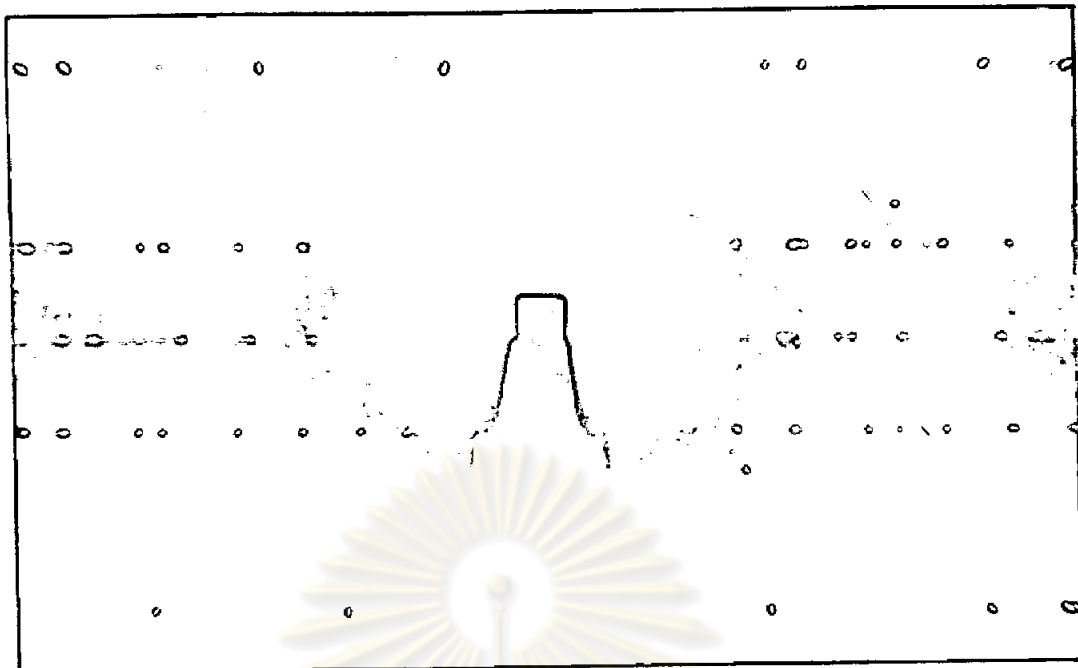


Fig. 4.10 Oscillation photograph of [001] as rotation axis,
CuK_α- radiation. Exposed 24 hr.

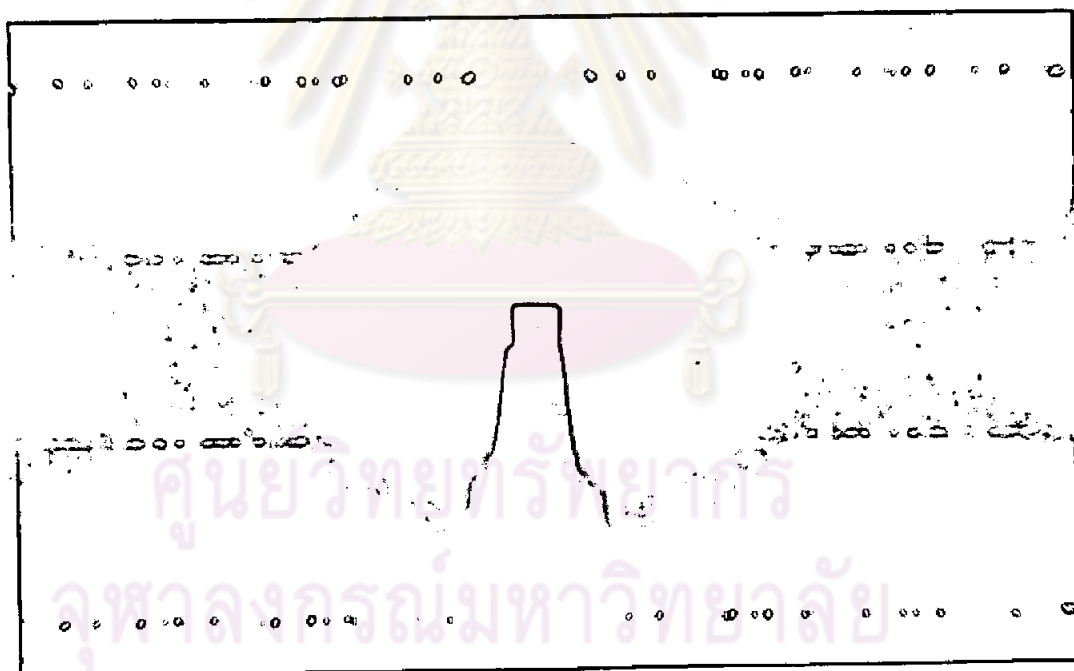


Fig. 4.11 Rotation photograph of [001] as rotation axis,
CuK - radiation. Exposed 24 hr.

Fig. 4.9 shows that diffusion streaks appear when k is odd while sharp spots appear when k is even. In addition, the Weissenberg photographs of $W_3V_5O_{20}$ (rotation axis "b") using $Mo K_\alpha$ -radiation also give fade diffusion streaks when k is odd. In the later work, therefore, the intensity data were collected by the Nonius Weissenberg camera when k was even only.

The length of rotating axis is found by using the Eq.

$$t = \frac{m \cdot \lambda}{\sin \tan^{-1} (y_m/r)} \quad \dots\dots\dots 4.3$$

where "t" is the lattice constant along the rotation axis, "m" is an integer, " λ " is the wavelength of X-ray beam, " y_m " is the height of the m th layer and "r" is the radius of the Weissenberg camera.

From Eq. (4.3) the two rotation axes, "b" and "c" were determined in Table 4.5 and table 4.6 respectively.

Table 4.5 Determination of the lattice constant, b, from [010] rotation photograph, $2\gamma = 57.3$ mm. $\lambda = 0.71068 \text{ \AA}$

layer	$2y$ (mm)	y (mm)	$\tan \nu = \frac{y}{\gamma}$	$\sin \nu$	$y_n = \lambda / \sin \nu$	b(Å)
1	5.50	2.750	0.0959	0.0954	7.400	7.40
2	11.25	5.625	0.1963	0.1927	3.670	7.38
3	17.00	8.500	0.297	0.284	2.500	7.49
4	23.75	11.875	0.414	0.383	1.860	7.43
5	31.00	15.500	0.541	0.476	1.490	7.47
6	40.25	20.125	0.702	0.575	1.240	7.42
7	51.00	25.500	0.665	0.554	1.069	7.48
8	67.00	33.500	1.169	0.758	0.937	7.49
						$b_{ave} = 7.45$

Table 4.6 Determination of the lattice constant, c , from [001] rotation photograph, $2\gamma = 57.3$ mm., $\lambda = 1.5418$ Å

layer	$2y$ (mm)	y (mm)	$\tan\gamma = \frac{y}{\gamma}$	$\sin\gamma$	$y_n = \lambda / \sin\gamma$	Å
1	24.25	12.125	0.4232	0.3897	3.9564	3.956
2.	71.25	35.625	1.2435	0.7793	1.9785	3.957
						$c_{ave} = 3.957$

The Laue photographs

The Laue method is a device for studying crystals by the incidence of X-rays along a given direction. A consequence is that a Laue photograph shows the symmetry of this direction. This is an important advantage of the method because it allows one to recognize elements of symmetry in the crystal by direct inspection of the photograph and to determine the Laue group to which the crystal conforms. In order to be able to accomplish this, more than one Laue photograph must be taken. To establish Laue symmetry, the incident X-ray beam must be directed along crystal direction of high symmetry.

For Laue method, the crystal is stationary, the orientation of each lattice plane is fixed in the polychromatic X-ray beam. From Bragg condition, the reflection angle θ is fixed for each set of planes and thus for a set of planes of spacing d_{hkl} , the value of $2d_{hkl} \sin\theta$ is also fixed and the only variables are "n" and " λ ". Now "n" must be an integer, and therefore the set of planes can reflect only specific components of white beam, of wavelength $\lambda_1, \lambda_2, \lambda_n$, such that

$$1\lambda_1, 2\lambda_2 = n\lambda_n = 2d_{hkl} \sin \theta$$

This relation is designated as

$$\lambda_1 = 2d_{hkl} \sin \theta$$

$$\lambda_2 = 2d_{2h,2k,2l} \sin \theta$$

$$\lambda_n = 2d_{nh,nk,nl} \sin \theta$$

and is equivalent to stating that the various orders of reflections which emanate from a set of planes are given off at the same angle and form only one Laue spot. This limits the usefulness of the Laue method for the determination of systematically missing reflections, hence space group.

In this experiment, one of the crystals was mounted along "c" as rotation axis, Laue photographs were taken along [100] and [010] axes by using Nonius precession camera with Mo radiation. These photographs were shown in Fig. 4.12. For the crystal mounted along "b" as rotation axis, a Laue photograph was taken along [001] axis by using Nonius Weissenberg camera of diameter 57.3 mm., with Mo-radiation. The three Laue photographs described above were used to determine Laue symmetry of tungsten-vanadium-oxide.

Weissenberg photographs

The serious disadvantage of rotation and oscillation methods is that the information which is contained in an entire two-dimensional reciprocal lattice plane is condensed into a one-dimensional layer line. Indexing reflections becomes very tedious and many films are necessary to avoid possible overlap of spots. K. Weissenberg recognized

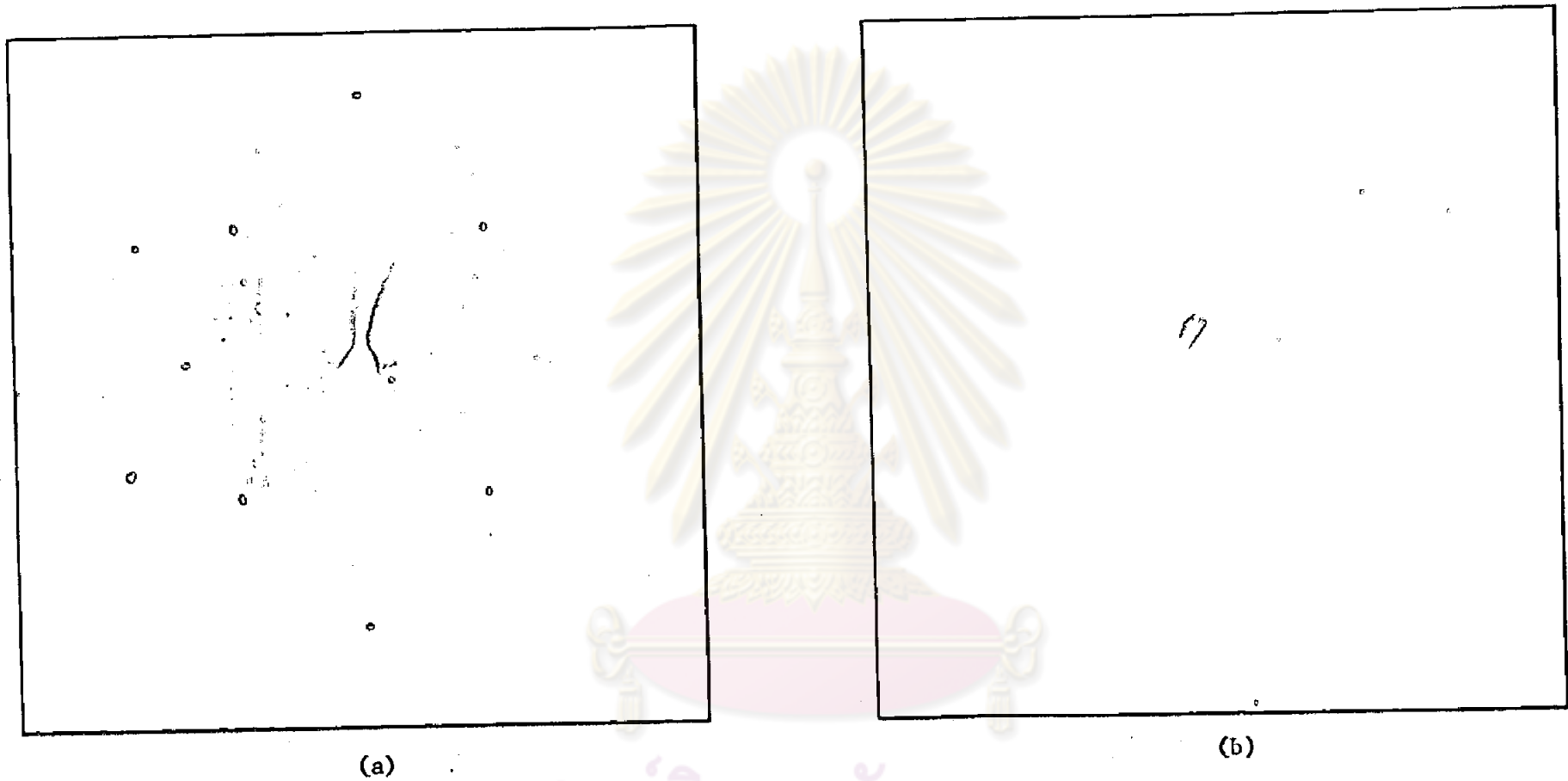
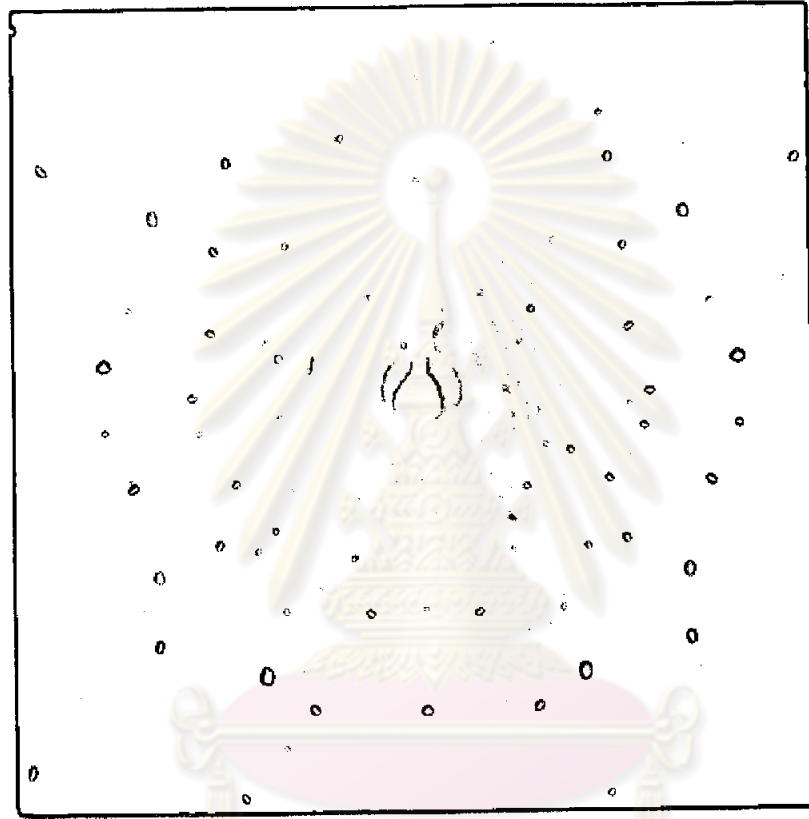


Fig. 4.12 (a) [100] Laue photograph Cu-radiation. Exposed 72 hr.
(b) [010] Laue photograph Mo-radiation. Exposed 54 hr.



(c)

Fig. 4.12 [001] Laue photograph with Mo-radiation. Eposed 54 hr.

ศูนย์วิจัยทรัพยากร
จุฬาลงกรณ์มหาวิทยาลัย

this problem and devised a new recording method known as the Weissenberg method which is similar to the rotation method in that a selected axis of the crystal is oriented to coincide with the axis of the cylindrical film. A single layer line is selected by a slotted screen which stops all other diffracted beam (Fig. 4.13) as the crystal is rotated the film is moved past the slot and reflections which occur at different times are recorded at different points on the film. The result of this is to spread the diffraction spots of the layer line over the two-dimensions of the film. A Weissenberg photograph gives two cell constants, the angle between them and the indices of reflections and symmetry.

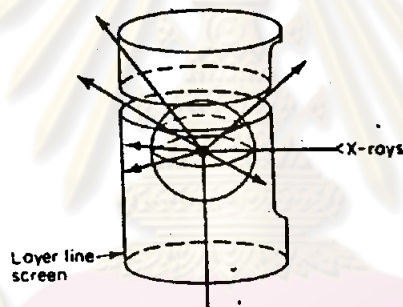


Fig. 4.13 Weissenberg layer line screen and its use.

For zero layer Weissenberg photograph, the incident X-ray beam is normal to the rotation axis and only zero layer line is allowed to reach the film. The method of recording an upper level for obtaining the photographs similar to zero-level one is known as the equi-inclination method because the undeviated beam and the diffracted beams such as OP_1 of Fig. 4.14 are inclined at the same angle to the reciprocal levels. The angle is equal to the angle of inclination μ , through which the rotation axis must be pivoted to bring the point p_1 onto

the surface of the sphere. Two instrumental settings must be determined for each equi-inclination upper level photograph.

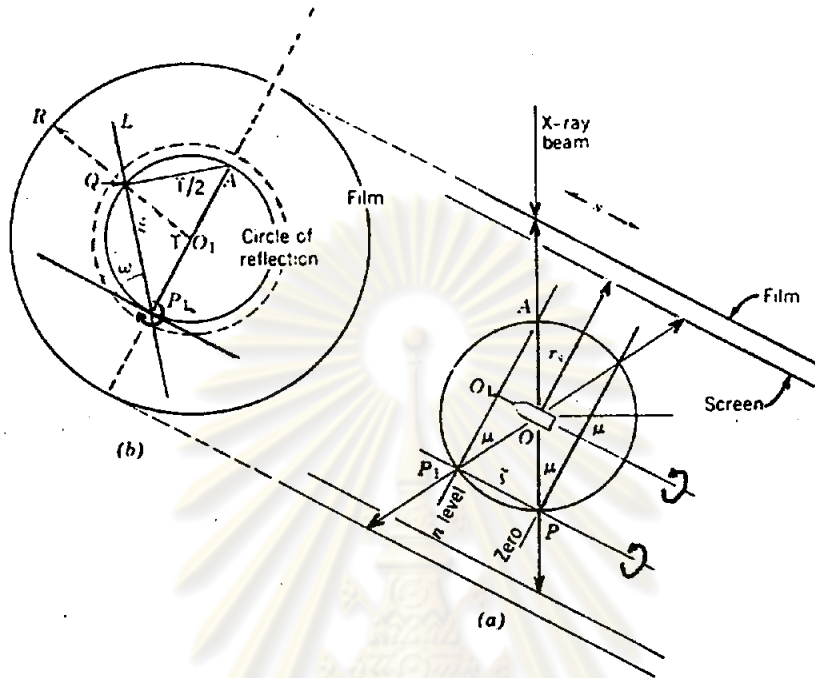


Fig. 4.14 Equi-inclination method of recording upper levels.

The inclination angle From Fig. 4.15 is

$$\mu = \sin^{-1} \left(\frac{PP_1}{AP} \right) = \sin^{-1} \left(\frac{\xi_n}{2} \right) \dots\dots\dots 4.7$$

Fig. 4.15 shows the arrangement, of cylindrical film and Ewald sphere in a rotation method and it follows that ξ_n (in r.l.u.) is given by

$$\frac{\xi_n}{1} = \frac{y_n}{\sqrt{R^2 + y_n^2}} = \sin \tan^{-1} \left(\frac{y_n}{R} \right) \dots\dots\dots 4.8$$

where ξ_n is the perpendicular distance between the zero and n^{th} levels of r.l. points

$$\xi_1 = \frac{\xi_n}{n}$$

R is the true film radius (note that the usual figure of 57.3 mm. is a diameter) and y_n the distance on the film, in the same units, from the zero to the n th layer lines.

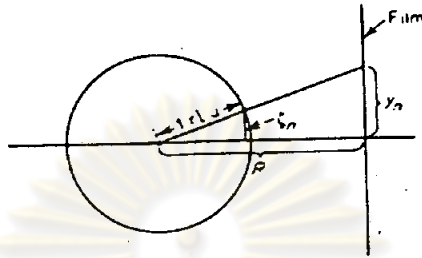


Fig. 4.15 Relation between ξ_n in the reciprocal lattice and spacing between the 0 and n th layer lines on a rotation photograph

From Eq. 4.7 and Eq. 4.8, Eq. 4.9 is obtained

$$\mu = \sin^{-1} \left[\frac{\sin \left\{ \tan^{-1} \left(\frac{y_n}{Y} \right) \right\}}{2} \right] \dots\dots\dots 4.9$$

The layer line screen setting, S , in Figure 4.14 shows the layer line screen in position to permit the reflections from a particular upper level to reach the film. The screen has been moved a distance of " S " mm from its zero-level position. The distance bears a simple relation to the radius of the screen (γ_s) and the inclination angle

$$S = \gamma_s \tan \mu \dots\dots\dots 4.10$$

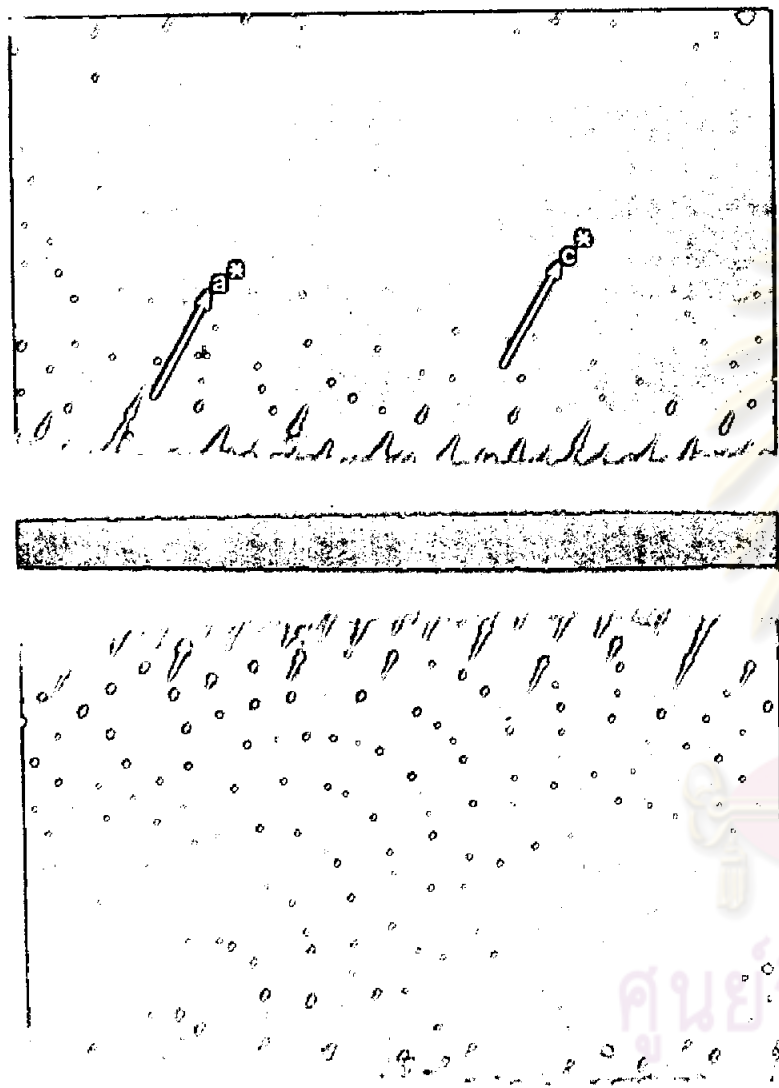
The slit's width of the layer line screen is usually adjustable. In practice the width is about 1.5 mm.

In this experiment, the two crystals correctly set by oscillation photographs were used to take Weissenberg photographs. The crystal mounted along the b-axis, was used to record Weissenberg photographs of the holand h21 layer for collecting intensity data by using Nonius Weissenberg camera with Zr-filtered MoK_α radiation and the multiple-film technique, with thin iron foils interleaved between successive film. From the zero layer Weissenberg photograph in Fig. 4.16 (a) the reciprocal axes and the interaxial angles are determined as shown in Table 4.7

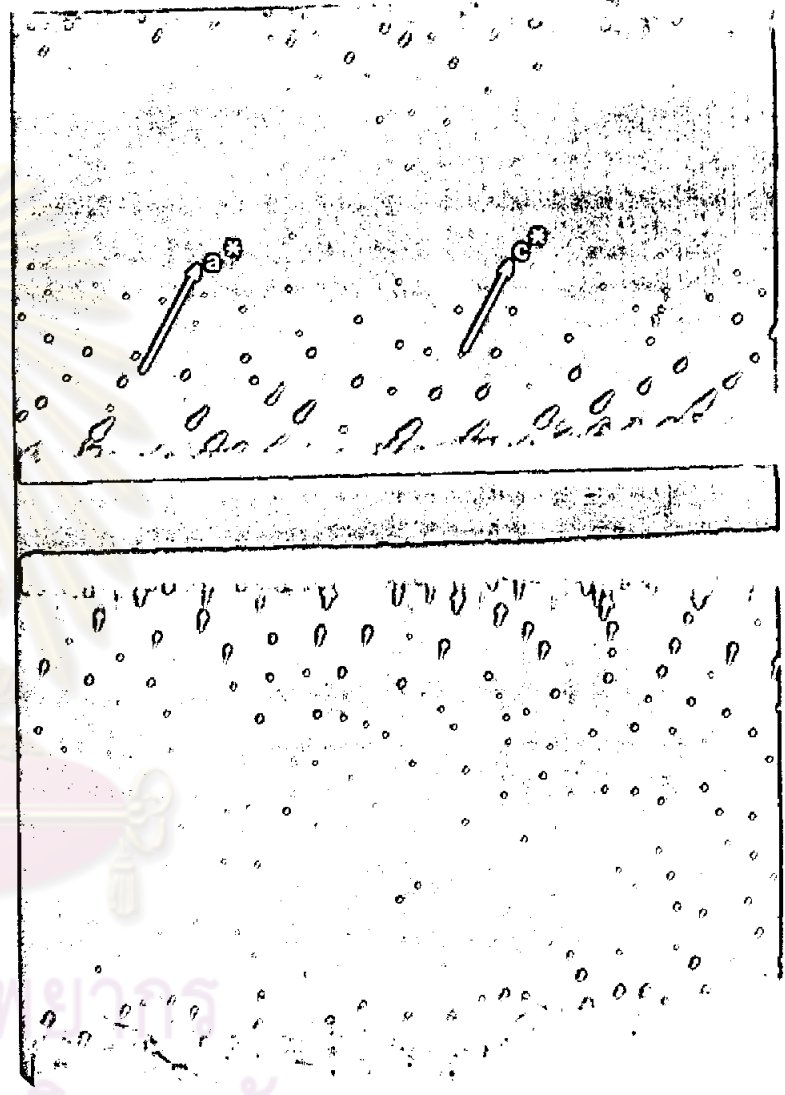
Table 4.7 Reciprocal axes and interaxial angles determined From the zero-level Weissenberg photographs

crystal rotation	reciprocal axis (r.l.u.)	reciprocal angle (degree)
b	$a^* = 0.291$ $c^* = 0.179$	$\beta^* = 89$
c	$a^* = 0.291$ $b^* = 0.0954$	$\gamma^* = 90$

The necessary parameters for taking the second layer photograph are listed in Table 4.8



(a)



(b)

Fig. 4.16 [010] Weissenberg photograph of $W_3V_5O_{20}$, MoK_{α} - radiation

(a) Zero layer (h0l) exposed 200 hr.

(b) Second layer (h2l) exposed 200 hr.

Table 4.8 The necessary parameters for second layer Weissenberg photograph, rotation axis b.

nth layer	$2y_n$ (mm.)	y (mm.)	y/γ_f	$\sin \mu$	μ	$\tan \mu$	$S=y \tan \mu$ (mm.)
2	11.25	5.625	0.1963	0.0963	5.5268	0.0968	2.47

For the crystal mounted along c axis the Weissenberg photographs of $hk1-hk2$ layer lines (Fig. 4.17) were recorded by using Nonius Weissenberg camera with Ni-filtered Cu K_α radiation. The reciprocal axes and the interaxial angles from the zero-level Weissenberg photographs are determined as shown in Table 4.7

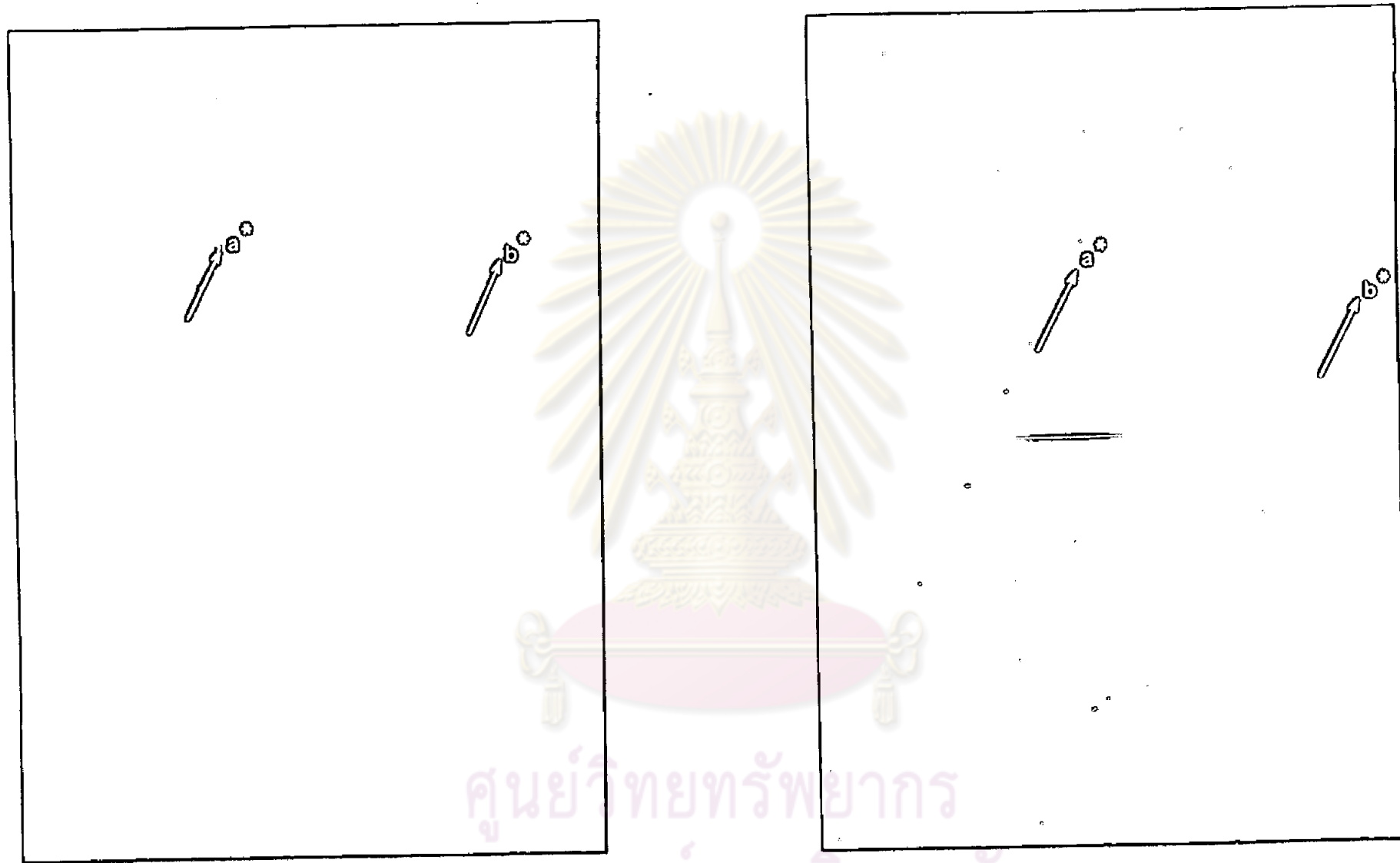
The necessary parameters for taking the first and second layer photographs are listed in Table 4.9

Table 4.9 The necessary parameters for [001] Weissenberg photograph

n th layer	$2y_n$ (mm.)	y (mm.)	y/γ_f	$\sin \mu$	μ	$\tan \mu$	$S=y \tan \mu$ (mm.)
1	24.25	12.125	0.4232	0.1949	11.24	0.1987	5.066
2	71.25	35.625	1.243	0.3896	22.93	0.4231	10.788

The intensities were estimated visually by comparison with a calibrated intensity scale obtained by timed exposures of one reflection from the crystal

From the [010] and [001] Weissenberg photographs, the reciprocal lattice nets were constructed as shown in Fig. 4.18



(a)

(b)

Fig. 4.17 [001] Weissenberg photograph of $W_3V_5O_{20}$, CuK_{α} - radiation.

(a) First layer (hk1) exposed 54 hr.

(b) Second layer (hk2) exposed 72 hr.

Intensity-data collection

For monoclinic crystal rotated about "b" axis, two blocks of data needed for collecting are hkl and $\bar{h}kl$ regions. In this experiment, multi-film equi-inclination Weissenberg technique was used to record intensities on zero and second layers using MoK_α -radiation. The Weissenberg photographs of every layer were taken twice with exposure time 200, and 6.34 hours using three films each time and thin iron foils placed between successive films. The intensity data of 469 independent reflections were obtained of which are 238 reflections for hol , $\bar{h}ol$ and 231 reflections for $h2l$, $\bar{h}2l$ data.

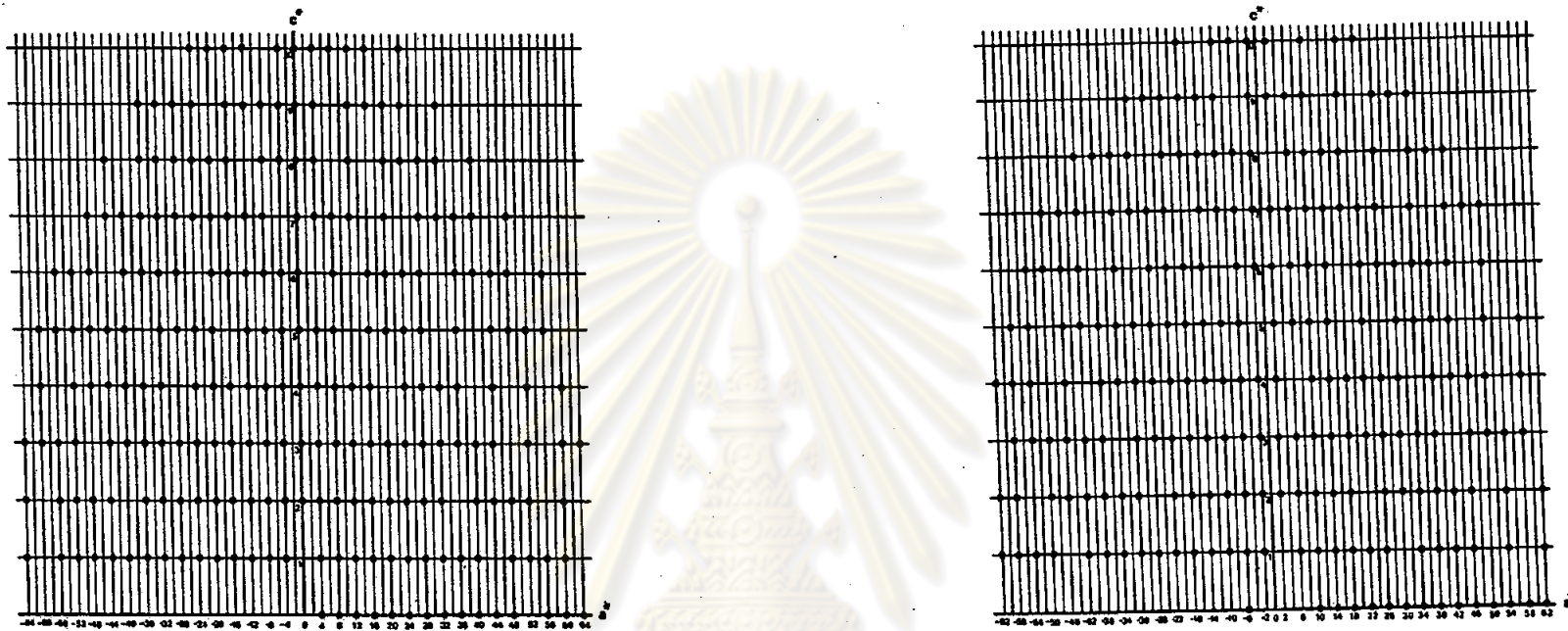
Measurement of intensity

The current methods of estimating blackening for film method may be divided into two classes, visual and photometric. In this experiment, intensity data obtained from measurements on Weissenberg films were measured by visual techniques. The visual estimation of spot darkening was the original technique for estimation of intensities from films and has been very successful. The usual method of measurement involves the systematic comparison of the observed reflections against a calibrated density scale. The spot scale should be uniformly dense region and has about the same size as the spots on the films. For this experiment, the 802 reflecting plane was selected as a standard spot. The calibrated intensity scale was prepared by timed exposures of the 802 reflection from the crystal using the Weissenberg method. The crystal rotation was limited to oscillate 2 degrees. The film was shifted 2 mm. between each exposure so as to be sure that the second reflection does not overlap the background of the first. The exposure times of the density steps

differed by 20% from the lowest to highest values. To perform the measurements, the film was placed on a light box and the intensity scale was placed over it. The reflection was viewed through any background on the scale strip. The reflection was compared with various reference spots until a match was found or until it was determined to fall between values. The appropriate value was assigned as the observed intensity.

Precession photographs

Precession method invented by Prof. M.J. Buerger is a Flat plate moving-film moving-crystal method which produces undistorted pictures of a chosen layer of a reciprocal lattice. The area of reciprocal space which is reproduced on the film is much more limited than that produced by Weissenberg method and for this reason the two cameras are usually used in conjunction. Precession method has an important application in the confirmation of space group symmetry. It is an extension of the oscillation method in which the crystal is made to oscillate about two mutually perpendicular axes both at right angles to the primary X-ray beam. By causing the flat film to follow the same motions as the crystal, an undistorted image is obtained. The two oscillations are produced 90° out of phase to each other, and with equal angle μ (the inclination angle) coaxial with the X-ray beam. In order to register a reciprocal-lattice net, its plane must be set parallel to the plane of the film, that is, normal to the X-ray beam when the inclination angle is set at zero. Such a net plane and its parallel upper layers will each intersect the Ewald sphere in a circle subtending a diffraction cone, and the desired layer is selected by means of an annular layer-line screen of appropriate dimensions fixed



(a)

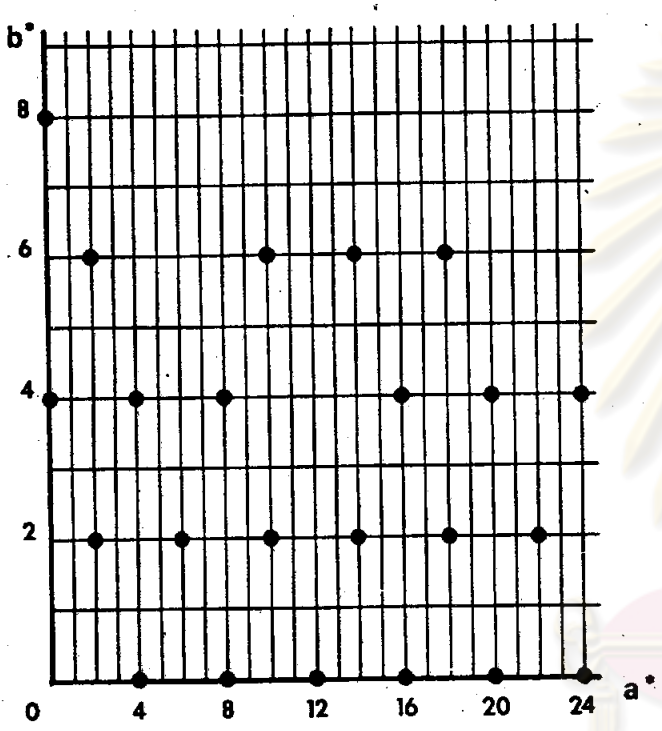
(b)

Fig. 4.18 The reciprocal lattice nets,

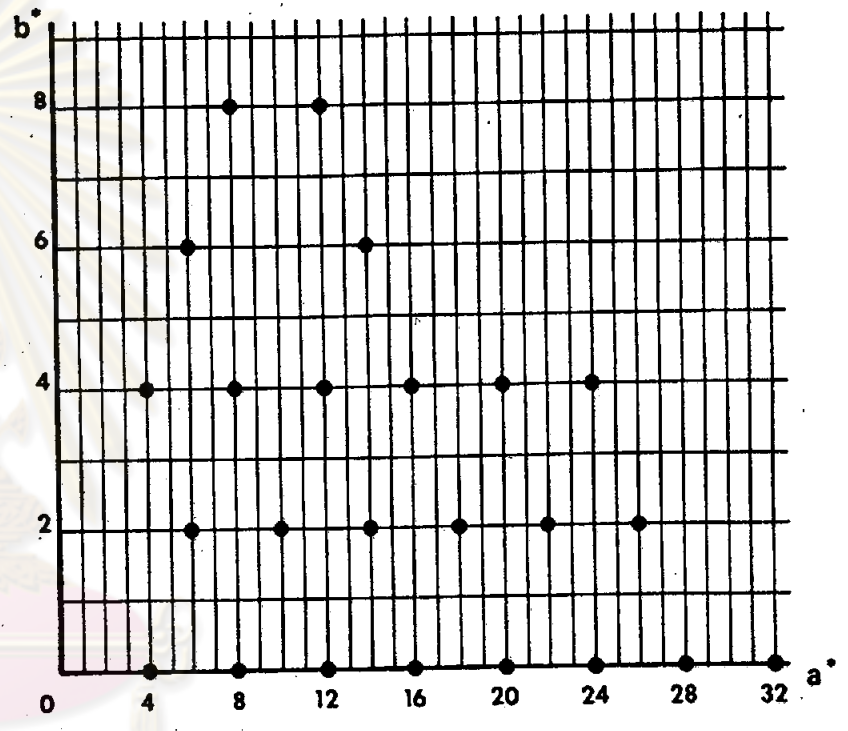
(a) Zero layer (h0l) [010] as rotation axis

(b) Second layer (h2l) [010] as rotation axis

ศูนย์วิจัยทรัพยากรธรณี
จุฬาลงกรณ์มหาวิทยาลัย



(c)



(d)

Fig. 4.18 (continued) The reciprocal lattice nets,

(c) First layer $-(hk1)$ $[001]$ as rotation axis

(d) Second layer $(hk2)$ $[001]$ as rotation axis

ศูนย์วิทยทรัพยากร

จุฬาลงกรณ์มหาวิทยาลัย

$$\frac{P'Q'}{PQ} = \frac{OP'}{OP} = \frac{OP'}{1} = F \quad \dots\dots\dots 4.11$$

where OP' or F is the crystal-to-film distance in mm, and therefore the distance between reciprocal lattice points PQ is

$$PQ = \frac{1}{F} \cdot P'Q' \quad \dots\dots\dots 4.12$$

Consequently, F is the magnification factor of the record.

The arrangement for recording the first level is shown in Fig. 4.21

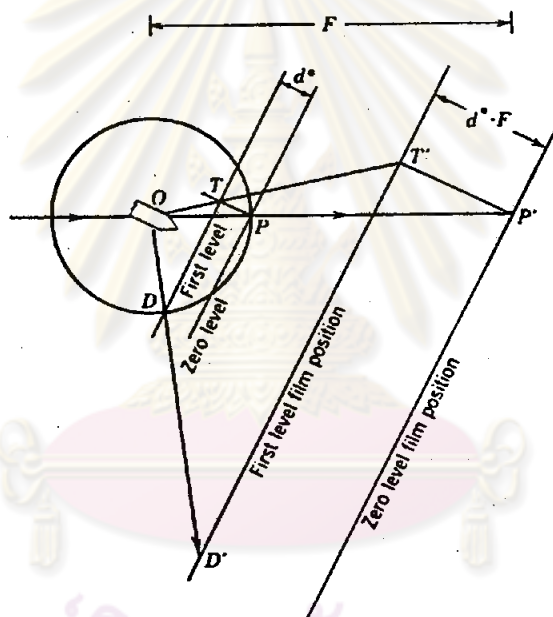


Fig. 4.21 Relation between zero- and first-level film positions

When the film is in position to record the zero level, its center is at P' , a distance F from the crystal. The center of that portion of the first level which moves through the sphere is at T , a distance $PT = d^*$ along the normal to the plane through P . If the scales of the zero- and first-level records are to be identical, the film must be moved along its normal a distance $F \cdot d^*$ to T' (The second

level requires the film to be displaced a distance $2d^*.F$ from the zero-level position). The validity of this statement can be shown by reference to a lattice point D on the first level, reflecting to D' on the film. From similar triangles $OP'T'$ and OPT

$$OT'/OT = OP'/OP = F \dots\dots\dots 4.13$$

In order to make a diffraction pattern, several settings are required, as follows :

1. The inclination (oscillation) angle $\bar{\mu}$
2. The annular layer-line screen radius r_s , usually available in fixed sizes of 15, 20, 25 and 30 mm.
3. The layer-line screen-to-film distance "S"
4. The displacement of the film from the center of precession $d^*.F$ (o for the zero layer)

For an upper-level pattern the height of the layer above the origin " d^* " in r.l.u. must be known, but otherwise all these quantities are independent of crystal parameters and are given by the relation

$$S = r_s \cot \cos^{-1} (\cos \bar{\mu} - d^*)$$

The value d^* is given by

$$d^* = \lambda/P$$

where P is the axial length in the direct lattice, parallel to the precession axis. The axial lengths can be determined by rotation method.

Precession photographs are used in crystal-structure analysis for two chief purposes : first, to permit symmetry observations leading

to determination of the space group, and measurements leading to a knowledge of the dimensions of the unit cell, and second, to provide data for the measurement of the intensities of the $|F_{hkl}|$'s. In this experiment the photographs are considered only for space-group and unit-cell determination.

Cell dimensions can be established easily and quickly by measuring the angles between any desired rows of the reciprocal lattice which lie in the plane of the precession photograph and the r.l. spacing in r.l.u. between any such rows, may be determined from Eq. 4.12

$$PQ = \frac{1}{F} \cdot P'Q'$$

where F is 60 mm. $P'Q'$ in mm. is measured from zero level photograph so reciprocal lattice PQ is obtained and at last the direct cell is determined

In this experiment Nonius precession camera of size $125 \times 125 \text{ mm}^2$ and the two crystals which had been already aligned on a Weissenberg camera were used for taking precession photographs by using MoK_α radiation. For the crystal mounted along "c", the "b" axis was first set parallel to the beam using 10° precession angle, unfiltered radiation and no screen. The zero and second level precession photographs (Fig. 4.22) were taken by using 30° precession angle, Zr-filtered MoK_α radiation. The necessary parameters for taking these photograph are listed in Table 4.10. After rotating the "b" axis 90° , the "a" axis was set parallel to the beam and precession photographs were recorded with same procedure as mentioned above. The necessary parameters for taking zero and first level photographs (Fig. 4.23) are listed in Table 4.11

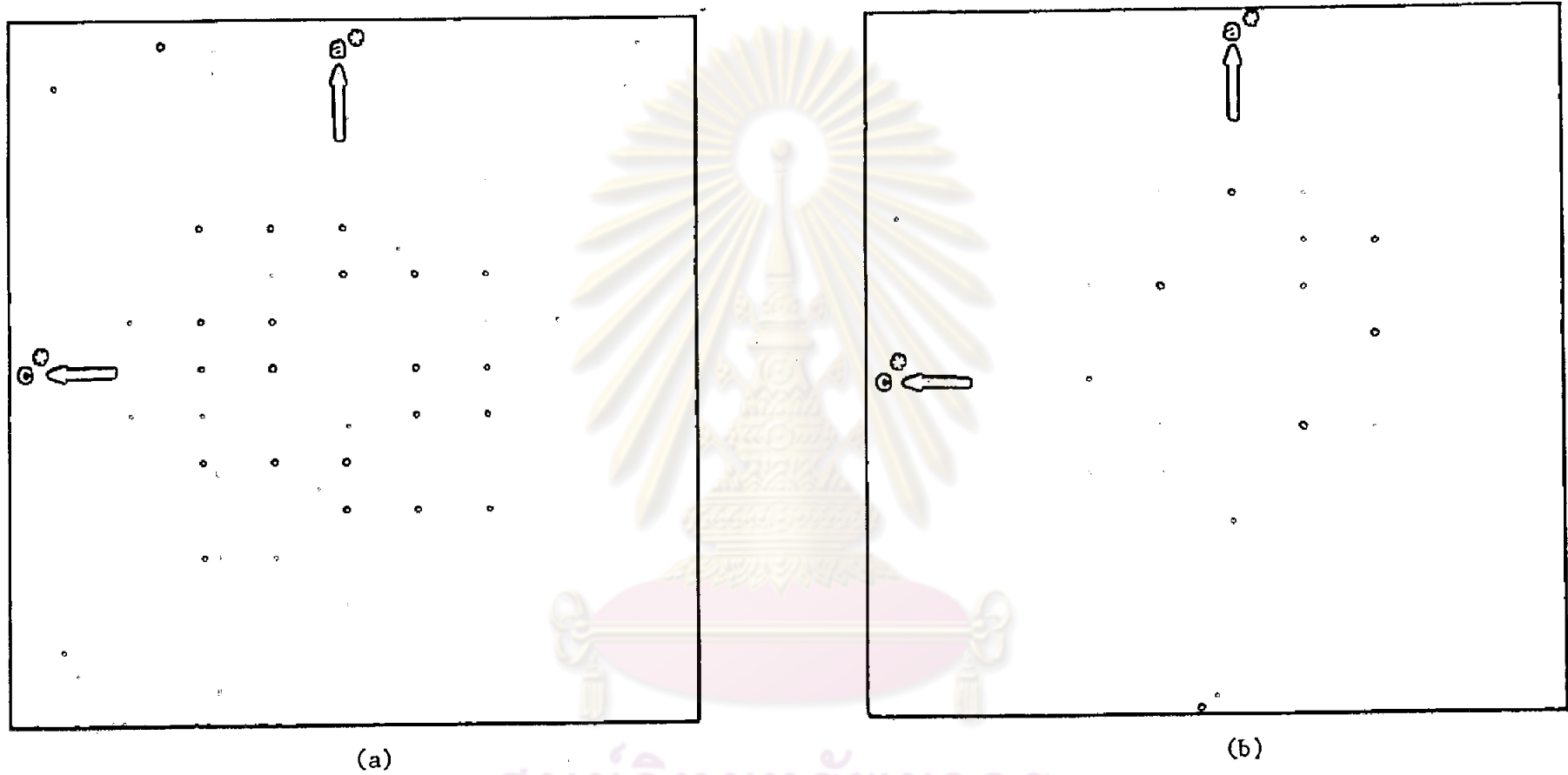


Fig. 4.22 Precession photograph of $[010]$ as precession axis, MoK_α -radiation.

(a) Zero layer, exposed 100 hr.

(b) Second layer, exposed 100 hr.

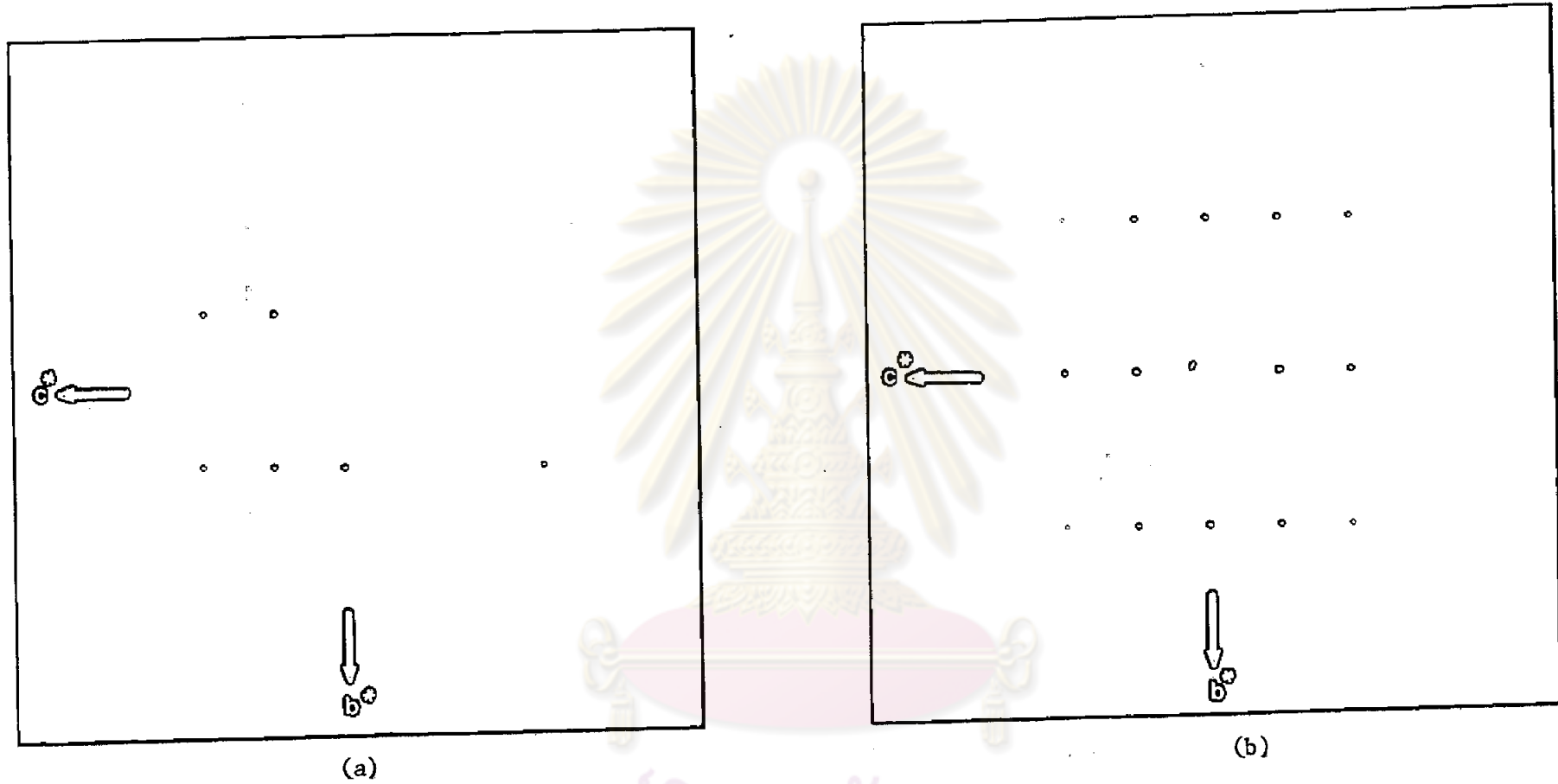


Fig. 4.23 Precession photograph of [100] as precession axis, MoK_α - radiation.

(a) First layer, exposed 100 hr.

(b) Zero layer, exposed 100 hr.

Table 4.10 The necessary parameters for taking [010] precession photographs. The value of b was taken from Table 4.5 :
"b" rotation axis.

n th layer	$F \cdot d_n^* = \frac{60 \times n \lambda}{b}$ (mm.)	$\bar{\mu}$ (degree)	r_s	$S = r_s \cot [\cos^{-1} \{ \cos 30 - d_n^* \}]$ (mm.)
0	0	30	15	26.0
1	11.4	30	30	27.5

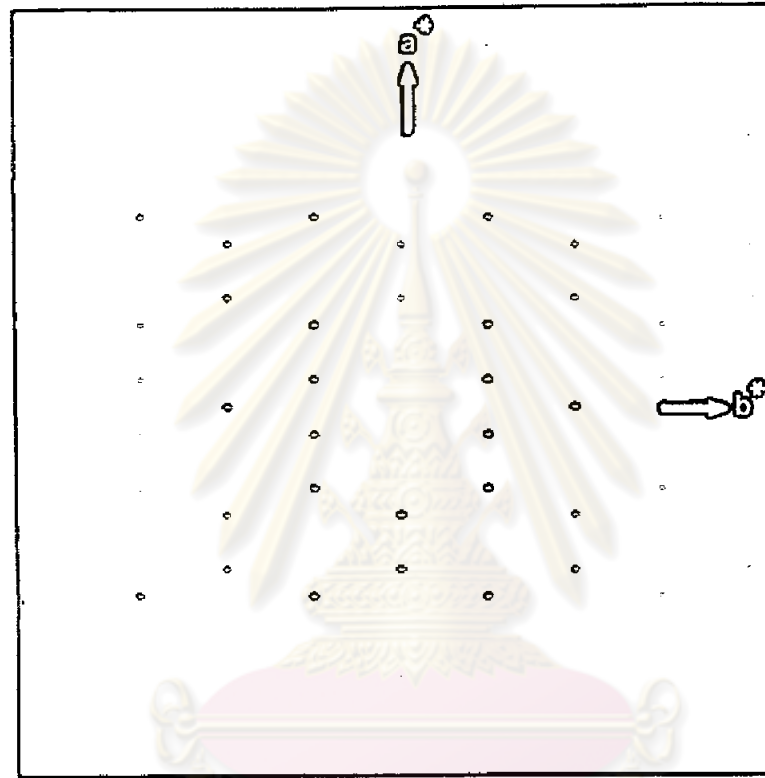
Table 4.11 The necessary parameters for taking [100] precession photographs. The value of a^* was taken from [010] Weissenberg photograph

n th layer	$F \cdot d_n^* = 60 \times n \lambda a^*$ (mm.)	$\bar{\mu}$ (degree)	r_s	$S = r_s \cot [\cos^{-1} \{ \cos 30 - d_n^* \}]$ (mm.)
0	0	30	15	26.0
1	3.5	30	15	23.1

The procedure which was explained above was repeated with the crystal mounted along b axis. The zero level photograph was taken by using c axis as a precession axis. The necessary parameters for taking a zero photograph are listed (Fig. 4.24) in Table 4.12

Table 4.12 The necessary parameters for taking [100] precession photographs. The value of c was taken from table 4.6 :
"c" rotation axis

n th layer	$F \cdot d_n^* = \frac{60 \times n \lambda}{c \sin \beta}$ (mm.)	$\bar{\mu}$ (degree)	r_s	$S = r_s \cot [\cos^{-1} \{ \cos 30 - d_n^* \}]$ (mm.)
0	0	30	15	26



ig. 4.24 Precession photograph of [001] as precession axis,
MoK_α- radiation. Exposed 100 hr.

จุฬาลงกรณ์มหาวิทยาลัย

Reciprocal lattice nets of precession photographs of Figure 4.22, 4.23, and 4.24 are drawn in Fig. 4.25.

From zero level photographs using "b", "a" and "c" axes as precession axes, the reciprocal axes and the interaxial angles were obtained in Table 4.13

Table 4.13 The reciprocal axes and the interaxial angles obtained from precession photographs

precession axis	reciprocal axis (r.l.u.)	reciprocal angle (degree)
b	a* = .0291 c* = .179	$\beta^* = 89$
a	b* = .0954 c* = .179	$\alpha^* = 90$
c	a* = .0291 b* = .0954	$\gamma^* = 90$

Determination of Unit Cell Dimensions

Preliminary unit cell dimensions of $W_3V_5O_{20}$ were determined from oscillation, rotation, Weissenberg and precession photographs, passed through the reciprocal lattice constants. From the symmetry of reflections shown in Laue, oscillation and precession photographs it is obvious that the crystal system of $W_3V_5O_{20}$ is monoclinic. The reciprocal lattice constants can be converted to the direct lattice by the formula

$$a = \frac{\lambda}{a^* \sin \beta^*}$$

$$b = \frac{\lambda}{b^*}$$

$$c = \frac{\lambda}{c^* \sin \beta^*}$$

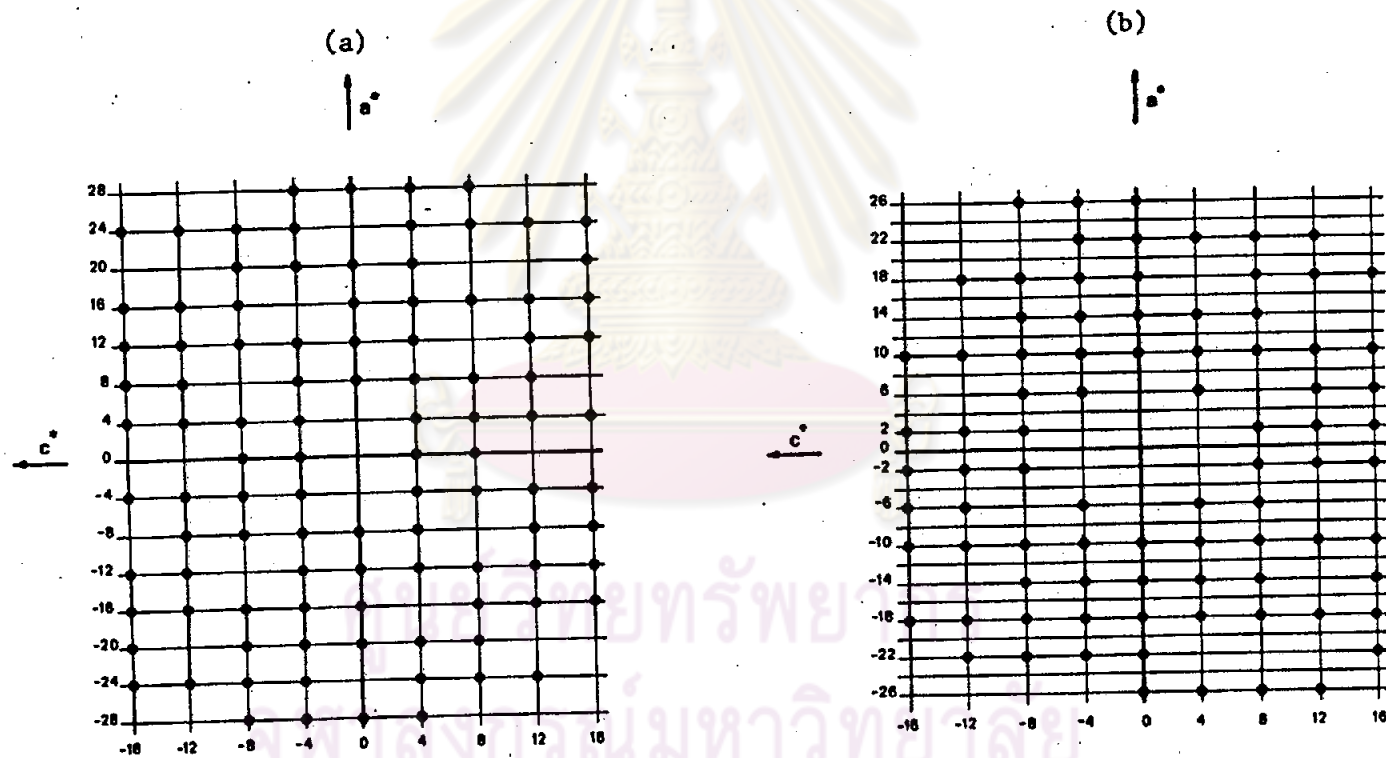
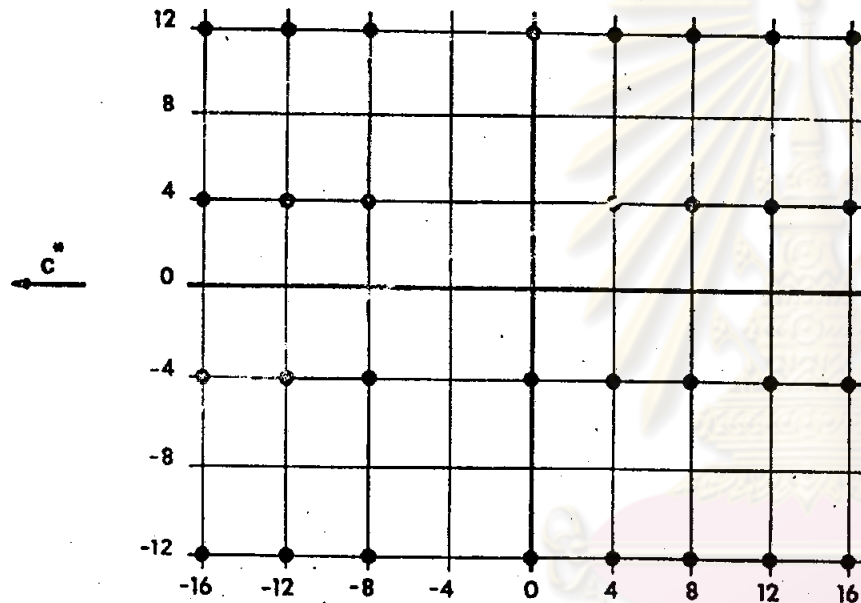


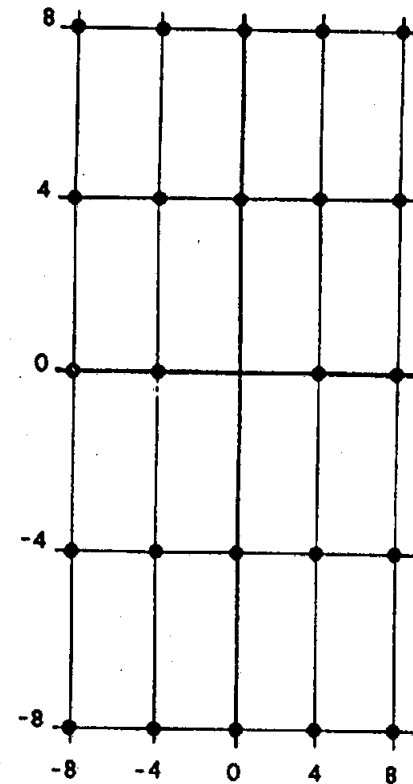
Fig. 4.25 Reciprocal lattice nets of precession photographs

(a) zero layer, $[010]$ as precession axis

(b) second layer, $[010]$ as precession axis



(c)



(d)

Fig. 4.25 (continued) Reciprocal lattice nets of precession photographs

(c) zero layer, $[100]$ as precession axis

(d) second layer, $[100]$ as precession axis

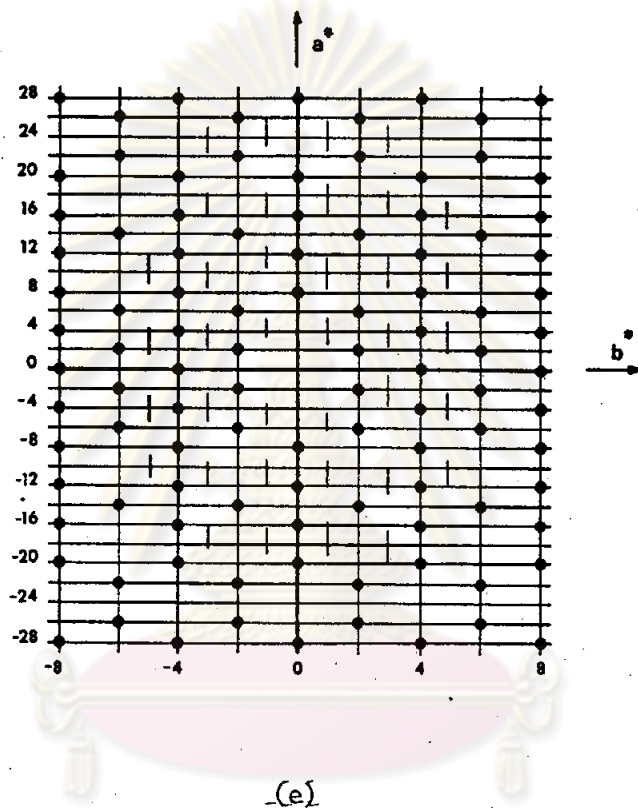


Fig. 4.25 (continued) Reciprocal lattice nets of precession photographs
 (e) zero layer, $[001]$ as rotation axis.

ศูนย์วิทยาศาสตร์
 จุฬาลงกรณ์มหาวิทยาลัย

$$\alpha = \beta = \gamma = \alpha^* = \beta^* = \gamma^* = 90^\circ$$

$$\beta = 180^\circ - \beta^*$$

The unit cell dimensions of $W_3V_5O_{20}$ are shown in Table 4.14

Table 4.14 Unit cell dimensions of $W_3V_5O_{20}$

reciprocal lattice	direct lattice
$a^* = .0291$ r.l.u. $\alpha^* = 90^\circ$	$a = 24.42 \text{ \AA}$ $\alpha = 90^\circ$
$b^* = .0954$ r.l.u. $\beta^* = 89^\circ$	$b = 7.45 \text{ \AA}$ $\beta = 91^\circ$
$c^* = .179$ r.l.u. $\gamma^* = 90^\circ$	$c = 3.97 \text{ \AA}$ $\gamma = 90^\circ$

Number of Formula Unit Per Cell

The number of formula unit per cell were calculated from the formula

$$Z = \frac{D_{\text{obs}} \times V \times N}{M}$$

- where
- Z = the number of formula unit per cell
 - D_{obs} = observed density = 5.10 g/cm^3
 - V = cell volume after refinement = $718.194 \times 10^{-24} \text{ cm}^3$
 - N = Avogadro's number = $6.02 \times 10^{23} \text{ (g}\cdot\text{mole)}^{-1}$
 - M = Molecular weight = 1126.24 atomic mass unit

The value of calculated "Z" is 1.96 However, Z must be an integer, so Z=2 and hence the calculated density = 5.21 g/cm^3

Space Group

Fig. 4.16, 4.17, 4.22, 4.23, 4.24 and Table 4.15 show that the conditions for the systematic presence of reflections correspond to three possible space groups $C2$, Cm , $C2/m$.

Table 4.15 Conditions for the systematic presence of reflections of $W_3V_5O_{20}$ crystal.

Reflections	Condition for systematic presence of reflections	Interpretation	Symbol
hkl	$h+k = 2n$	Centered on the C-Face(001)	C
hol	no condition for all values of l	-	-
oko	no condition	-	-

ศูนย์วิทยทรัพยากร
จุฬาลงกรณ์มหาวิทยาลัย